Preface

This master thesis was conducted at Nofima AS, division for Food in the group Raw Materials and Processing at Ås, Norway, from August 2012 to May 2013. Supervisors at Nofima were Sissel B. Rønning and Mona E. Pedersen, while Vincent Eijsink was the appointed liable supervisor at UMB. This work was supported by grants from the Fund for Research Levy on Agricultural Products in Norway and the Norwegian Research Council (203697/O99).

The first spark of interest for this thesis came at an open presentation of master theses at UMB, where this particular thesis caught my eye as a very interesting way of connecting molecular and cell biology to food sciences. The entire course of study changed after accepting the thesis, needing to take a course at UiO, a UMB course as individual course and taking a course while conducting the master thesis. It all worked out in the end, and I am happy to have indulged in this project.

I would first and foremost like to thank my supervisors at Nofima, Sissel and Mona, for their continual guidance, help and go-ahead spirit in both professional and casual scenarios. Thanks go to Vincent as well, for providing some guidance in the writing process. I would also like to thank Jacob Torgersen and Vibeke Høst for help with immunofluorescence microscopy and general lab assistance, respectively.

Final thanks go to my girlfriend, for her support and advice, and for enduring this past year at Pentagon.

Ås, May 14. 2013

Petter V. Andersen

I

Table of Contents

Abstract

Post-mortem tenderisation of meat is a complex process, of which all the details are far from understood. Cell death by apoptosis is recently proposed as a novel mechanism in this process. The main aim of this study was to investigate if bovine satellite muscle cells, cultivated *in vitro,* would induce apoptosis when oxygen was removed from the incubation medium.

Satellite muscle cells was seeded out in Entactin-Collagen IV-Laminin (ECL) coated culture wells and allowed to differentiate before oxygen was removed by adding EC-Oxyrase® to the differentiation medium (DM). Muscle cells were incubated without oxygen for 2h, 4h, 6h and 22h. Samples were analysed by immunofluorescence microscopy, quantitative real-time PCR, western blot, caspase 3/7 assay, caspase 9 assay and viability assay.

Evident signs of actin filament depolymerisation and actin degradation following oxygen removal were observed. Tubulin filaments depolymerised soon after oxygen removal, while the tubulin monomers was unchanged. The mRNA expression of the pro-apoptotic protein Bim increased significantly at all times investigated, as did the mRNA of caspase-independent apoptosis inducing factor (Aif). Mitochondrial membrane potential decreased significantly at 6h after oxygen removal. Concentration of protective Hsp-70 and PARK7 protein seemed to increase transiently, with maximum concentrations at 2h and 4h respectively. Concentration of caspase 9 decreased significantly at all times investigated, with a minimum concentration at 22h. Concentration of caspase 3/7 decreased significantly at 2h and 4h, before increasing gradually from 4h to 22h, ending with a concentration above the control sample. Viability of muscle cells increased at 2h, before decreasing gradually afterwards, ending in a significant decrease at 22h.

In conclusion, the results strongly indicated that satellite muscle cells induced apoptosis when oxygen was removed from the incubation medium, and that the mitochondrion was an important element in the apoptotic event.

Sammendrag

Mørning av kjøtt post-mortem er en kompleks prosess, og det er mange faktorer som påvirker den endelige mørheten i kjøtt. Celledød ved apoptose er nylig foreslått som en av mekanismene som kan påvirke mørningsprosessen. Hovedmålet i denne studien var å undersøke om satellittmuskelceller, dyrket *in vitro*, ville indusere apoptose når oksygen ble fjernet fra vekstmediet.

Satellittceller fra muskler av storfe ble sådd ut på Entactin-Collagen IV-Laminin (ECL)-belagte dyrkningsbrønner, hvor muskelcellene differensierte før oksygen ble fjernet ved å tilsette EC-Oxyrase® til differensieringsmediet. Muskelcellene ble satt til inkubasjon uten oksygen i 2t, 4t, 6t og 22t. Prøver ble analysert ved immunfluorescens mikroskopi, kvantitativ real-time PCR, western blot, caspase 3/7 assay, caspase 9 assay og viability assay.

Fjerning av oksygen ga tegn på en depolymerisering av actinfilamentene, og at actinmonomerer ble destruert. Tubulinfilamentene ble tydelig depolymerisert etter fjerning av oksygen, men tubulinmonomerene viste ingen tegn på destruksjon. mRNA uttrykk av det pro-apoptotiske proteinet Bim økte signifikant ved alle undersøkte tidspunkter, det samme gjorde mRNA uttrykket til caspaseuavhengig apoptose induserende faktor (Aif). Membranpotensialet til mitokondrier avtok signifikant 6t etter fjerning av oksygen. Konsentrasjonen av de beskyttende proteinene Hsp70 og PARK7 nådde en topp etter henholdsvis 2t og 4t etter fjerning av oksygen, før konsentrasjonen avtok igjen ved lengre inkubasjonstider. Konsentrasjonen av caspase 9 minket signifikant på alle undersøkte tidspunkter, med et minimum etter 22t. Konsentrasjonen av caspase 3/7 minket signifikant etter 2t og 4t, men økte igjen fra 4t til 22t, hvor konsentrasjonen etter 22t var høyere enn i kontrollprøven. Levedyktigheten til muskelcellene økte etter 2t, før den gradvis minket, og til slutt nådde en levedyktighet signifikant lavere enn kontrollen ved 22t.

Resultatene indikerte at satellittmuskelceller induserte apoptose når oksygen ble fjernet fra vekstmediet, og at mitokondriene spilte en viktig rolle i denne prosessen.

Abbreviations

AEBSF	4-(2-Aminoethyl) benzenesulfonyl fluoride
Aif	Apoptosis-inducing factor
Apaf-1	Apoptotic protease-activating factor 1
DM	Differentiation medium
DMEM	Dulbecco's Modified Eagle Medium
DMSO	Dimethyl sulfoxide
ECL	Entactin-Collagen IV-Laminin
ECM	Extracellular matrix
EDTA	Ethylenediaminetetraacetic acid
FBS	Fetal bovine serum
Hsp	Heat shock proteins
MRF	Myogenic regulatory factor
PARK7	Parkinson disease 7
PBS	Phosphate buffered saline
Pen Strep	Penicillin Streptomycin
PFA	Paraformaldehyde
PM	Proliferation medium
SD	Standard deviation
SDS	Sodium dodecyl sulphate

1. Introduction

1.1 Meat quality

Meat quality is a broad term that includes all factors related to the intrinsic properties and our subjective perception of quality. It includes diverse attributes such as health issues associated with contamination of the meat, carcass composition, production-related issues such as animal welfare, and eating quality including components such as tenderness, juiciness, colour and flavour (Maltin et al., 2003). Regarding eating quality, the most important trait is considered to be tenderness, and consumers are willing to pay more for tender meat than for any other quality attribute (Miller et al., 2001). The process of tenderisation is not fully understood, and this chapter focuses on some of the post-mortem changes that can influence final tenderness in meat.

1.1.1 Tenderness

There are three factors that determine meat tenderness; 1) background toughness, 2) the toughening phase, and 3) the tenderisation phase (Koohmaraie and Geesink, 2006). Tenderness is usually assessed by measuring the shear force needed to cut through a cooked meat sample, across the fibre direction, using a Warner-Bratzler protocol or a slice shear force protocol (Shackelford et al., 1999). The general view is that final tenderness is governed by post-mortem changes in meat, and may often outweigh the *in vivo* effects of feeding strategies and selective breeding, if executed optimally (Maltin et al., 2003). The well documented post-mortem events of major importance include the onset of *rigor mortis* and post-mortem proteolysis. There is some evidence supporting an event before onset of rigor, namely apoptosis, which can impact the overall proteolysis of muscle tissue (Ouali et al., 2006). The timeline of events post-mortem would then be cell death by apoptosis, followed by *rigor mortis,* ending with final enzymatic proteolysis (Figure 1.1). These events are in many ways interrelated and will be discussed in the following chapters.
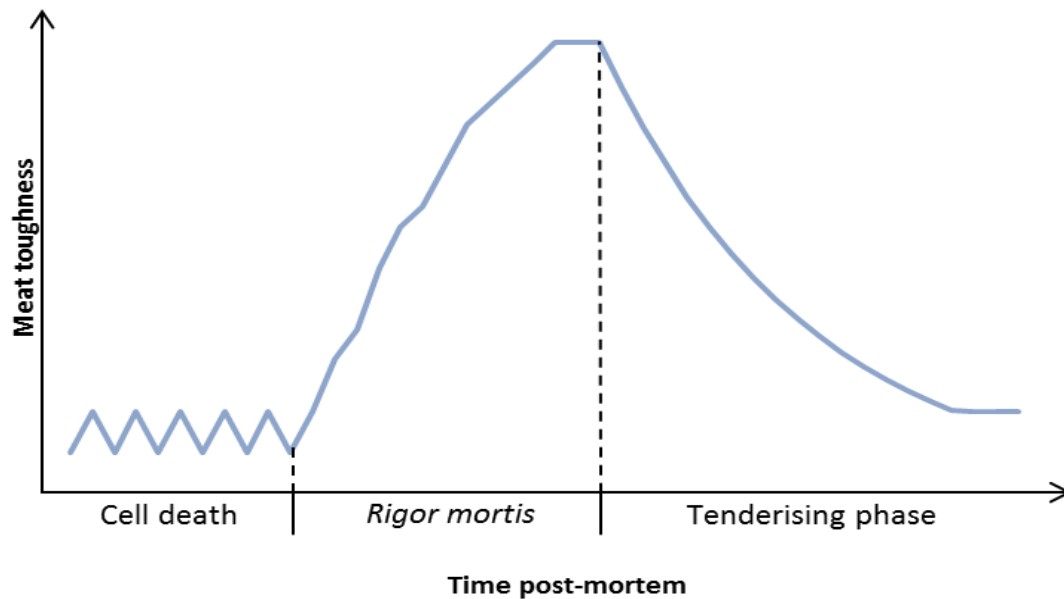
Figure 1.1: *Different phases determining the outcome of post-mortem tenderisation. Modified from Ouali et al. (2006).*

1.1.2 Apoptosis-mediated tenderisation

Evidence supporting the theory of apoptosis tenderisation is emerging, and recent studies try to elucidate this theory further. Apoptosis is a non-destructive way for cells to die and is characterized by cellular events such as shrinkage of cytoplasm membrane, cell separation, formation of apoptotic bodies, loss of mitochondrial membrane potential, activation of proteolytic caspases and inversion of cytoplasm membrane potential (see chapter 1.2 for details). Apoptosis theory of tenderisation has origin in the view that muscle cells has no option but to engage in a cell death mechanism post slaughter, presumably apoptosis, because the cells will be deprived of oxygen and nutrition after bleeding (Herrera-Mendez et al., 2006). Evidence from post-mortem muscle cells show that actin is degraded during the first 24 hours post exsanguination and that extracellular space increases with time during *rigor mortis,* which can be explained by cell shrinkage from apoptosis (Becila et al., 2010). Calcium concentrations in cytoplasm increases gradually during *rigor mortis*, due to emptying of the sarcoplasmic reticulum (Vignon et al., 1989), possibly affecting the mitochondrion. The mitochondrion will also be affected by other post-mortem conditions, most notably removal of oxygen, thus losing its capacity to oxidize molecular oxygen, giving an increase in the permeability of the outer membrane, which again leads to release of protein compounds from the intermembrane space and formation of free oxygen radicals (Herrera-Mendez et al., 2006). Ouali et al. (2006) reported that a pH plateau corresponding to inversion of membrane polarity during apoptosis can be

detected in post-mortem muscle, and that overexpression of Hsps from stress pre-slaughter, can give a negative impact on tenderness, possibly due to the anti-apoptotic effect of Hsps. There is also some evidence supporting a correlation between an increase in tenderness and increased degradation of mitochondria (Laville et al., 2009). There are also indications that the rate of apoptotic nuclei varies between different muscles, probably due to differences in muscle fibre types (Cao et al., 2010), meaning that apoptosis-mediated tenderisation can vary between muscle groups. Some of the casapases have calpastatin as a substrate, and can in this way impact tenderisation by increasing the overall calpain activity (Kemp and Parr, 2012). Cells have also been documented to induce apoptosis under hypoxia, as documented in cultured lymphoma cells in 0.16 % oxygen (Muschel et al., 1995).Taken together, there are numerous findings supporting a role of apoptosis in post-mortem tenderisation and it would explain the often observed issue that the first few hours after slaughter are essential for meat tenderisation (Herrera-Mendez et al., 2006). On the other hand, there is still lacking direct evidence that caspases contribute significantly to post-mortem tenderisation (Bowker et al., 2010), but this may be caused by the lack of studies examining apoptosis in meat or muscle cell systems exclusively.

1.1.3 Rigor mortis

The change from muscle to meat is a lengthy process and can take as long as 48 hours in beef cattle. This process starts early post-slaughter when oxygen is depleted and metabolism switches from aerobic to anaerobic, which leads to production of lactic acid and gives a fall in pH from ≈ 7.1 to ≈ 5.6. The muscle cells will try to maintain normal function of ionic pumps, but this will fail when all ATP from the anaerobic processes is depleted. This lack of ATP will lead to an influx of calcium ions, and these two factors are responsible for irreversible cross-bridge formation between myosin and actin filaments, giving a substantial increase in meat toughness during *rigor mortis* (Juárez et al., 2012).

Changes in temperature post-mortem can greatly affect the events at onset of rigor. High temperatures when entering rigor, considered to be temperatures over 20 °C, will decrease pH, sarcomere length and protein solubility, and give an undesirably high shear force (Bruce and Ball, 1990). While the rapid decrease in pH is generally desired, the other negative impact of high temperatures during rigor outweighs the possible benefits of the pH drop. Post-mortem temperature of 15 °C under rigor seems to be optimal for tenderness, giving the lowest shear force measurements and least decrease in sarcomere length, when beef was subsequently aged at 4 °C (Devine et al., 1999).

When considering the effects of pH it's important to consider the effects of pH fall rate and the ultimate pH (pH_u), although their impact on tenderness is not fully understood (Maltin et al., 2003). The pH fall rate will naturally influence pH_u, and a rapid decline in pH is usually desired to give a low pH_u (Hannula and Puolanne, 2004). Meat with low (<5.8) or high (>6.3) pH_u will generally have the lowest shear force measurements (Purchas et al., 1999). The increase in shear force at intermediate (5.8≤pH_u≤6.3) pH_u can likely be attributed to a decrease in sarcomere length (Purchas and Aungsupakorn, 1993).

It is important to note that pH and temperature affects other aspects of meat quality, e.g. colour (Bruce and Ball, 1990), and should be accounted for when selecting a post-mortem treatment protocol.

1.1.4 Post-mortem proteolysis

Proteolysis of proteins responsible for muscle cell structural integrity is thought to be the cause of tenderisation post-mortem. There are three general criteria for a protease to be considered as a contributor to the tenderisation of meat; 1) the protease must be endogenous to the muscle cells, 2) it should be able to reproduce changes in myofibrils *in-vitro* under optimum conditions, and 3) the protease must have access to myofibrils in tissue (Koohmaraie, 1996). The only known proteolytic system that fulfils these three criteria is the calpain system (Koohmaraie, 1994).

1.1.4.1 The calpain proteolytic system

The major proteases of the calpain system are μ-calpain and m-calpain, which are Ca^{2+} dependent cysteine proteases with a pH optimum of 7.2-8.2 (Goll et al., 2003). μ-calpain seems to be the key protease in post-mortem proteolysis, and the major cause for variation in tenderness in meat where proteolysis is the major determinant of tenderness (Koohmaraie and Geesink, 2006). The calpains has been shown to cleave myofibril proteins in a specific manner to create polypeptides similar to those found during post-mortem tenderisation (Bowker et al., 2010). Calpastatin specifically inhibits the calpains, and it seems that this protein has no other substrates in muscle cells (Goll et al., 2003). Even though the calpain system is assuredly an important part of meat tenderisation, there is an emerging amount of evidence suggesting that multiple enzymes and interdependent muscle factors may influence post-mortem proteolysis and its link to tenderisation (Bowker et al. 2010).

1.2 Apoptosis

Apoptosis and necrosis are two different ways for cells to die. In apoptosis this happens without causing harm to surrounding cells, and is an important process for development and homeostasis in multicellular organisms (Kerr et al., 1972). Apoptosis transpires in a controlled manner, where the cell membrane stays intact until the cell can be phagocytized. Apoptotic cells change morphologically by; 1) separating from nearby cells; 2) condensation and fragmentation; 3) formation of apoptotic bodies; 4) shrinkage of cytoplasm membrane; and 5) exposure of surface molecules for recognition by phagocytes (Figure 1.2) (Kerr et al., 1972). Another hallmark of apoptosis, regardless of apoptotic pathway, is the inversion of membrane polarity as a part of the process of exposing surface molecules (Martin et al., 1995). Necrosis, on the other hand, causes swelling of cytoplasm and mitochondria, loss of membrane integrity, swelling of organelles and total cell lysis (Becila et al., 2010).

Figure 1.2: Simple diagram of morphological stages during apoptosis (Kerr et al., 1972).

1.2.1 Phases of apoptosis

The process of apoptosis can be divided into four stages: initiation, commitment, amplification and demolition. Each of these stages will be discussed chronologically in the following sections.

1.2.1.1 Initiation

Initiation of apoptosis can be divided into three different pathways; 1) activation of cell death receptors; 2) by stimuli that provoke general cellular damage or; 3) by exposure to cytotoxic cell granules (Figure 1.3) (Slee et al., 1999).
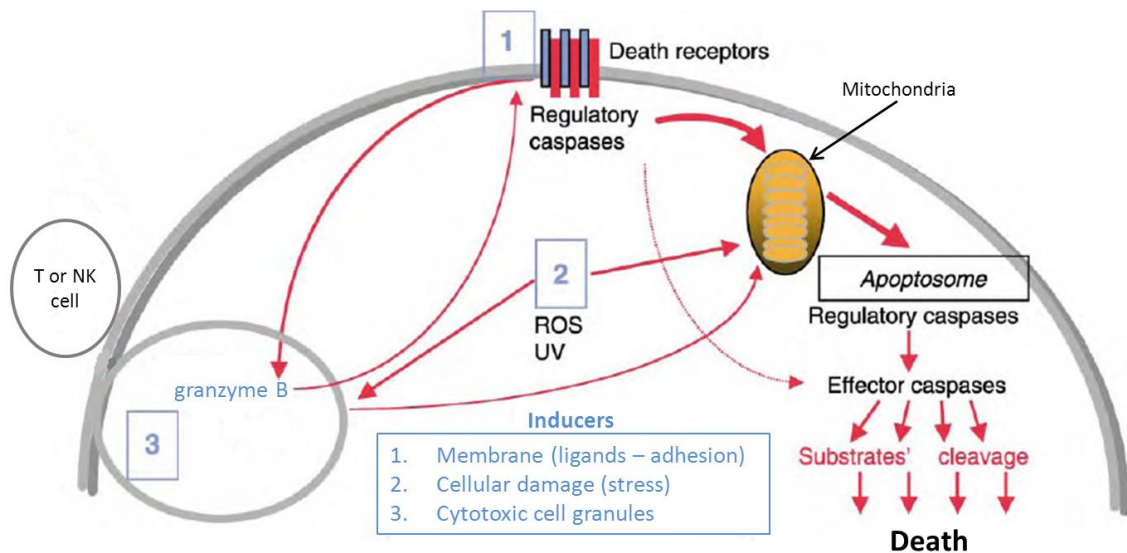
Figure 1.3: *Schematic overview of three different ways of initiating apoptosis in the cell. Modified from Nicholson et al. (2004) and Slee et al. (1999).*

The death receptors in the cell membrane are of a subset of the tumour necrosis factor (TNF) receptor family. They are activated by extracellular ligands, such as TNF ligands which is mainly produced by activated macrophages and monocytes (MacEwan, 2002), and this pathway is therefore known as extrinsic activation of apoptosis. These receptors contain a cytosolic domain responsible for recruiting adaptor molecules, which in turn recruits caspases to the receptor complex. Caspases are activated by cross processing them within the complex, creating active caspase dimers. Caspase 8 is known to be activated in this manner (Slee et al., 1999).

Another way of activating apoptosis is by the discharge of granules onto the cell surface by cytotoxic lymphocytes (T or natural killer cells), known as the "kiss of death". These granules contain proteases capable of cleaving and activating caspases. For example is granzyme B is known to cleave and activate most caspases, but the preferred substrate is caspase 3, which in turn activates other caspases to further the apoptosis process (Slee et al., 1999).

The last group of apoptosis initiation incorporates all other stimuli that can induce apoptosis, and these are regarded as intrinsic factors because the mitochondrion plays an important role in this

activation. There are many apoptosis-promoting stimuli in this category (e.g. radiation, heat shock and survival factor deprivation), and most of these stresses seem to exert their effects on the mitochondrion resulting in activation of the mitochondrial apoptosome (Slee et al., 1999).
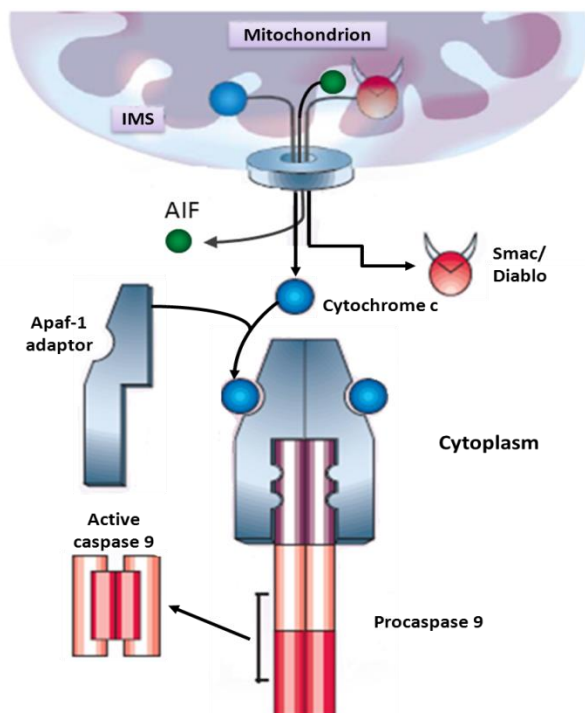
Figure 1.4: Proteins are released from the mitochondrion as a result of increased permeability. A detailed way of action for cytochrome c is also shown. Modified from Nicholson (2000).

1.2.1.2 Commitment

The commitment to apoptosis in mammalian cells most often arise from mitochondrial damage (Green, 2011). The damage exerted on the mitochondrion results in an increase in permeability of the mitochondrial membrane and subsequent release of proteins, such as Aif, cytochrome c and Diablo/Smac, of which all normally resides within the mitochondrion (Nicholson et al., 2004). Aif escapes the mitochondrion before cytochrome c (Cande et al., 2002), and Aif affect apoptosis in a caspase-independent manner by translocation to the nucleus from the mitochondrial intermembrane space, causing condensation of chromatin and digestion of DNA (Susin et al., 1999). Cytochrome c works in a caspase-activating manner by changing the conformation of cytosolic adaptor molecule Apaf-1, which in turn activates caspase 9 (Figure 1.4)

(Nicholson, 2000). The complex made out of Apaf-1, cytochrome c, procaspase 9 is known as the apoptosome, and it requires energy, in the form of ATP, to activate caspase 9 (Nicholson et al., 2004). Diablo/Smac is a mitochondrial cofactor protein that works by shutting down inhibitor-of-apoptosis (IAP) proteins, which is proteins that can down-regulate the activity of effector caspases, thus Diablo/Smac can ensure a full engagement of the proteolytic pathway (Nicholson, 2000).

1.2.1.3 Amplification

A cascade of caspase activation commences after activation of caspase 9, starting with the simultaneous activation of caspase 3 and 7. Caspase 3 can then activate caspase 2 and 6, which means that all effector caspases are active. In addition, caspase 8 and 10 are activated, creating an amplification of the overall caspase activation (Figure 1.5).All these caspases are not required for the cell to die, but most of them are probably required for the cell to engage in an apoptotic phenotype (Slee et al., 1999).
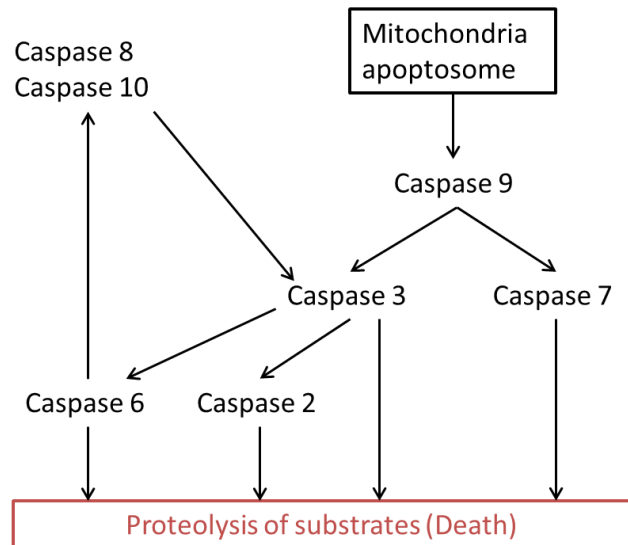
Figure 1.5: *Diagram of activation of caspases after formation of apoptosome. Modified from Nicholson et al. (2004).*

1.2.1.4 Demolition

When all the necessary caspases are activated, the final demolition begins. The caspases have over 1000 known substrates in the cell (Green, 2011), including among other calpastatin, Hsp90, actin and Bcl2 (Nicholson et al. 2004). Many of the caspases are localized in the cytosol, and many of their known substrates are located in the nucleus or other cellular compartments, creating a possible delay in activation of a caspase and its proteolytic attack (Slee et al., 1999).

1.2.2 Bcl2-family apoptotic proteins

Muscle cells contain genes for proteins which induce or inhibit apoptosis, and many of these proteins interact to determine if apoptosis is initiated. All these proteins share similarities with a protein named Bcl2, which is an important anti-apoptotic protein, but its exact mechanism of action is not known. The current theories of its function consider the binding of Bcl2 to an adaptor molecule, thus preventing caspase activation, or that Bcl2 binds to mitochondrial proteins, thus preventing the further release of pro-apoptotic molecules by maintaining the mitochondrial membrane potential (Vaux 2004). Kannan and Jain (2000) states that "Bcl2 protects cells against diverse cytotoxic insults, for example, gamma radiation, cytokine withdrawal, hypoxia, ROS, dexamethasone, staurosporine, and cytotoxic drugs", meaning that Bcl2 protects from a diverse range of cellular insults.

The Bcl2-like proteins can be divided into three families, which are classified by their homology with the four Bcl2 domains, designated BH1-4. Family 1 Bcl2-like proteins contain three or four

of the BH domains, Bcl-x and Bcl2 belongs to this family. Family 2 Bcl2-like proteins contain BH1-3, Bax and Bak are members of this family. Family 3 Bcl2-like proteins contain only the BH3 domain, Bim, Bid, Bad, and Bmf are examples of proteins from this family. Family 1 contains the anti-apoptotic proteins, while family 2 and 3 contains pro-apoptotic proteins. The pro-apoptotic proteins transduce apoptotic signals by binding to the anti-apoptotic proteins via their BH3 domain (figure 1.6), thus inactivating the anti-apoptotic potential of these proteins (Vaux 2004).
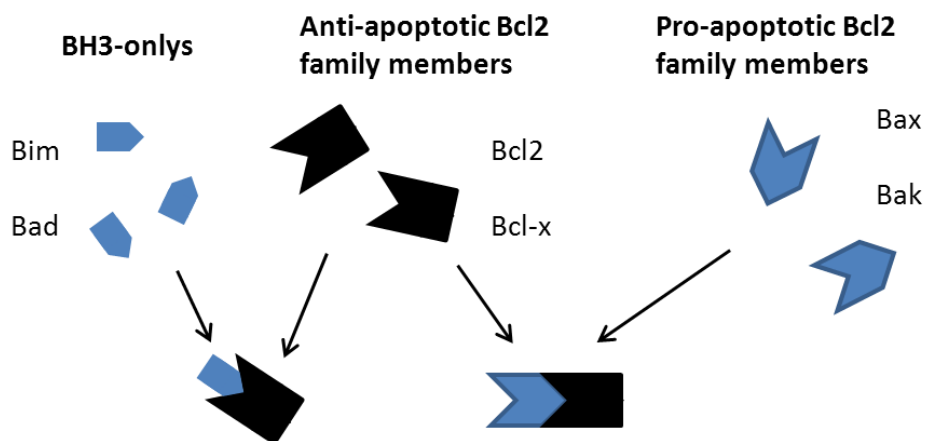
Figure 1.6: Proposed interactions of Bcl2-like proteins in apoptosis mechanisms. Modified from Vaux (2004).

1.2.3 The impact of calcium

Increased calcium concentrations in the mitochondrion can affect apoptosis by altering the outer mitochondria membrane permeability, thus releasing pro-apoptotic signals from inside the mitochondrion. An increase in permeability involves opening of permeability transition pores, which is made of a large protein complex, that is localised at the contact points between the inner mitochondrial membrane and the outer mitochondrial membrane (Crompton, 1999). This complex operates as a voltage dependent channel that becomes activated by high concentrations of Ca^{2+}, resulting in a persistent pore opening, allowing low-molecular-mass components (such as cytochrome c and Aif) to leave the mitochondrion (Orrenius et al., 2003).

1.2.4 Caspases

Caspases are cysteine proteases, which are enzymes that cleave after an aspartate residue, involved in the controlled cell death processes of apoptosis.

All the caspases share a similar structural composition, containing a prodomain, a large subunit and a small subunit. The prodomain regulates enzymatic activation, while the subunits are

required for an enzymatically active enzyme. To activate a caspase, the prodomain is removed and the two subunits rearrange to make a monomeric casapse, which in turn is activated by binding to an identical monomer, creating an active dimer (Figure 1.7). This reaction requires proteolytic cleavage of the three subunits, carried out by other endoproteases, which normally are other capases (Nicholson et al., 2004).
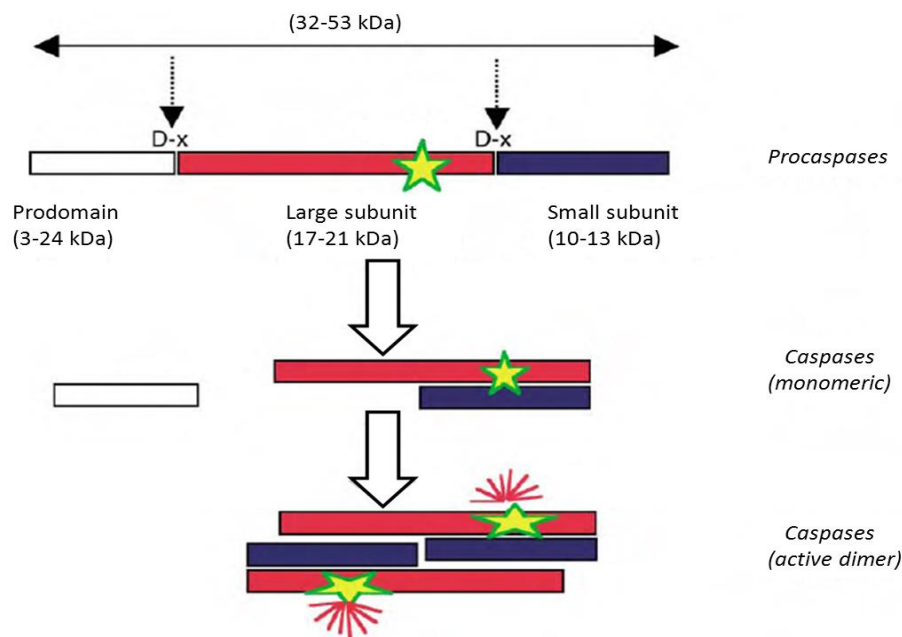
Figure 1.7: Schematic illustration of activation of caspases. The star represents the enzymatically active site of the caspase. Modified from Nicholson et al. (2004).

There are fourteen known caspases and they can be divided into three different groups. Group 1 includes caspases 1, 4, 5 and 11, which are involved in cytokine processing, and will not be further discussed because they are not directly involved in apoptosis. Group 2 includes caspases 3, 6 and 7, which have very short prodomains (<10 kDa) and are thought to be crucial in the effector phase of apoptosis. The short prodomains suggests that activation of these caspases is relatively simple. Group 3 consists of caspases 2, 8, 9 and 10, which have longer prodomains and are primarily thought of as regulation caspases. The remaining caspases (12, 13 and 14) are not well enough described to be grouped. Even though this is a simplification of the individual caspase functions, this grouping can be a good tool for further understanding their involvement in apoptosis (Slee et al., 1999).

1.2.5 The role of heat shock proteins and PARK7 in apoptosis

Hsps can protect against both extrinsic and intrinsic apoptosis pathways (Beere, 2005). Hsp27, Hsp70 and Hsp90 subfamilies have been associated with protection from a wide variety of apoptosis inducing factors, such as UV radiation (Simon et al., 1995), death receptor ligation (Mehlen et al., 1996), heat shock (Mosser et al., 2000), and nutrition withdrawal. The exact mechanism of protection from Hsps in these scenarios is difficult to identify, because of a complex regulation of the apoptotic pathway as a whole (Beere, 2005). Hsps can impact intrinsic apoptosis by inhibiting the mitochondrial release of cytochrome c (Mosser et al., 2000) and they can inhibit the function of Bid (Gabai et al., 2002) and Bax (Gotoh et al., 2004). Hsp70 is also shown to interact with Aif, negating its apoptotic effect outside the mitochondrion (Ravagnan et al., 2001).

PARK7, also known as DJ-1, is another protective protein of which exact function is not yet known (Hauser and Hastings, 2013). PARK7 has the ability to oxidize and translocate to mitochondria in response to oxidative stress, thus serving a role as sensor and protector against toxicity from oxidative stress (Canet-Aviles et al., 2004). A deficiency in PARK7 is shown to give a seemingly normal accumulation of reactive oxygen species during oxidative stress, but the cells are not able to cope with prolonged toxicity, leading to cell death by apoptosis (Martinat et al., 2004). PARK7 is also shown to affect apoptosis by decreasing Bax expression and inhibiting caspase activation (Fan et al., 2008).

1.3 Muscle development

Muscle cells are, as all other cells in mammalian cells, of eukaryotic nature and share their structural features. Muscle cells are surrounded by a plasma membrane which encapsulate all other cellular components, such as organelles, the cytoplasm and cytoskeletal structures. Organelles are membrane enclosed subunits with specific functions, separated from the rest of the cytoplasm. The nucleus and mitochondrion are examples of different organelles in eukaryotic cells. The cytoskeleton, on the other hand, is in direct contact with the cytoplasm. Actin, desmin and tubulin are classified as cytoskeletal filaments, and are important in the cell for movement and cellular integrity, among other things (Lodish et al., 1996).

In addition, the cells have complex genetic programs controlling their development and cell cycle, e.g. specific muscle differentiation factors to determine the fate of a given muscle cell. This chapter describes important traits of myogenesis, the mitochondrion and the cytoskeleton in muscle cells.

1.3.1 Myogenesis

This section describes the functions and roles of some important regulatory proteins related to proliferation and differentiation, in addition to an overview of the different cell stages that occur from satellite muscle cells to differentiated muscle cells. Each of the discussed regulatory proteins will be described by how they affect the aforementioned stages in cell life.

1.3.1.1 Cell stages

Muscle cells have a remarkable capability of self-renewal and repair *in vivo*. These processes make use of quiescent satellite muscle cells, which can be activated later in the life of the living animal.

The quiescent muscle satellite cells lie under the basal lamina of muscle cells and are activated by muscle injury or signals from microvasculature or inflammatory cells (Danoviz and Yablonka-Reuveni, 2012). They subsequently enter the cell cycle, starting by proliferating and/or migrating to places injury (Bischoff and Heintz, 1994). The initial activity of satellite cells are controlled by expression of Pax3 or Pax7 genes (Relaix et al., 2006). The satellite cells develop into myoblasts, which can proliferate further, before they differentiate into multinucleated myotubes (Lodish et al., 1996). The activated satellite cells can also be designated to replenish the satellite cell pool, by re-entering the quiescent stage, to ensure that the satellite cell pool do not diminish (Danoviz and Yablonka-Reuveni, 2012). The different cell stages, from satellite muscle cells to maturing muscle, are controlled by the myogenic regulatory factors, which are activated at different stages of myogenesis (Figure 1.8).
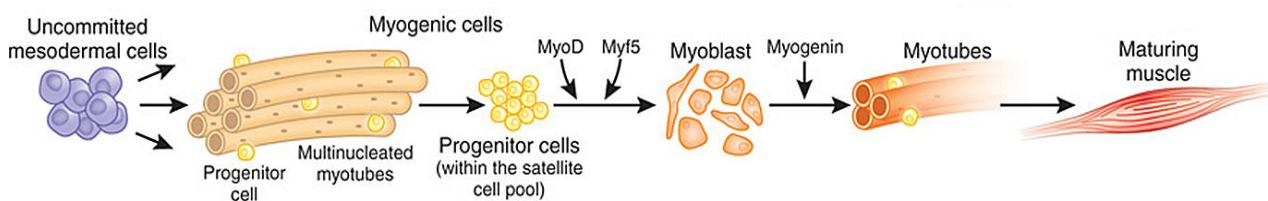
Figure 1.8: *Formation of muscle from uncommitted mesodermal cells to maturing muscle, where three of the myogenic regulatory factors are showed at their stage of interaction. Modified from Hettmer and Wagers (2010).*

1.3.1.2 Myogenic regulatory factors

The MRFs orchestrate gene expression during myogenesis, in collaboration with other muscle-specific and general factors. The MRFs are DNA-binding proteins containing a basic helix-loop-

helix domain, which efficiently binds to promoters and enhancers of muscle-specific genes (Berkes and Tapscott, 2005). There are four MRFs that regulate determination and differentiation of skeletal muscle cells; MyoD, Myf5, myogenin and MRF4.

MyoD and Myf5 are both required for multi-potential mesodermal cells to commit to myogenesis, called "commitment" factors, since an absence of these genes results in no formation of skeletal myoblasts and knockout mice lacking both these MRFs die short time after birth (Rudnicki et al., 1993). Either of the two working separately contributes to an apparently normal myogenic development (Berkes and Tapscott, 2005). In addition to the influence on myoblast commitment, MyoD might act as a molecular switch that turns on cell differentiation by affecting cell cycle regulators (Jin et al., 2007) and it can have an important role in regulating the size of the muscle satellite cell pool (Kanisicak et al., 2009). In addition, Pax3 and Pax7 genes can affect the activation of MyoD in adults, thus they too affect myogenesis without being characterized as MRFs (Relaix et al., 2006). MRF4 is expressed both early, during myogenic commitment, and later in the cell cycle, during differentiation (Berkes and Tapscott, 2005). It is therefore thought that MRF4 can affect both commitment and differentiation, but the primary role of MRF4 might be that it accelerates cell proliferation and to some degree inhibit differentiation, by suppressing MyoD expression, to ensure enough cells are available for a successful myogenesis processes to take place (Jin et al., 2007). The fourth MRF, myogenin, is a critical protein for muscle cell differentiation, myocyte fusion, maturation of myofibres and muscle growth, and the protein is shown to be essential during pre-natal development (Meadows et al., 2008).

1.3.2 Cytoskeleton

There are three cytoskeletal filaments; microfilaments, microtubules and intermediate filaments. These filaments are named after their relative diameter when polymerised. Microfilaments are smallest with a diameter of 7 nm, intermediate filaments are in the middle with a diameter of 10 nm and microtubules are largest with a diameter of 24 nm (Lodish et al., 1996).

1.3.2.1 Microfilaments

The microfilament of major importance in muscle cells is actin, which was first identified in muscle cells, where it makes out the thin filaments needed for energy dependent muscle contraction. Actin filament dynamics impacts features such as cell motility, cell shape, and the interaction of a cell with its surrounding cells or extra cellular matrix (ECM). The dynamics of actin assembly is regulated by actin-binding proteins (ABP), known as capping proteins and

severing proteins. Capping proteins affects the growth and/or depolymerisation rates of the filament they bind, while the severing proteins enhance fragmentation (Maiti and Bamburg, 2004).

Actin assembly is carried out as a molecular self-assembly process, where bound ATP is hydrolysed to ADP following assembly, via an ADP + P_i intermediate. The growing actin filament is made out of a barbed end and a pointed end (Figure 1.9). As the actin monomers assemble into a filament, the cytoplasmic concentration of actin monomers decreases. This results in a release of monomers from the pointed end, which in turn can assemble at the barbed end. This happens because the barbed end has a higher affinity for actin monomers than the pointed end. The exchange of actin monomers from the pointed end to the barbed end under steady-state is called treadmilling. The process requires energy in the form of ATP, which in turn gives rise to movement of the actin filament within the cytoplasm (Maiti and Bamburg, 2004).
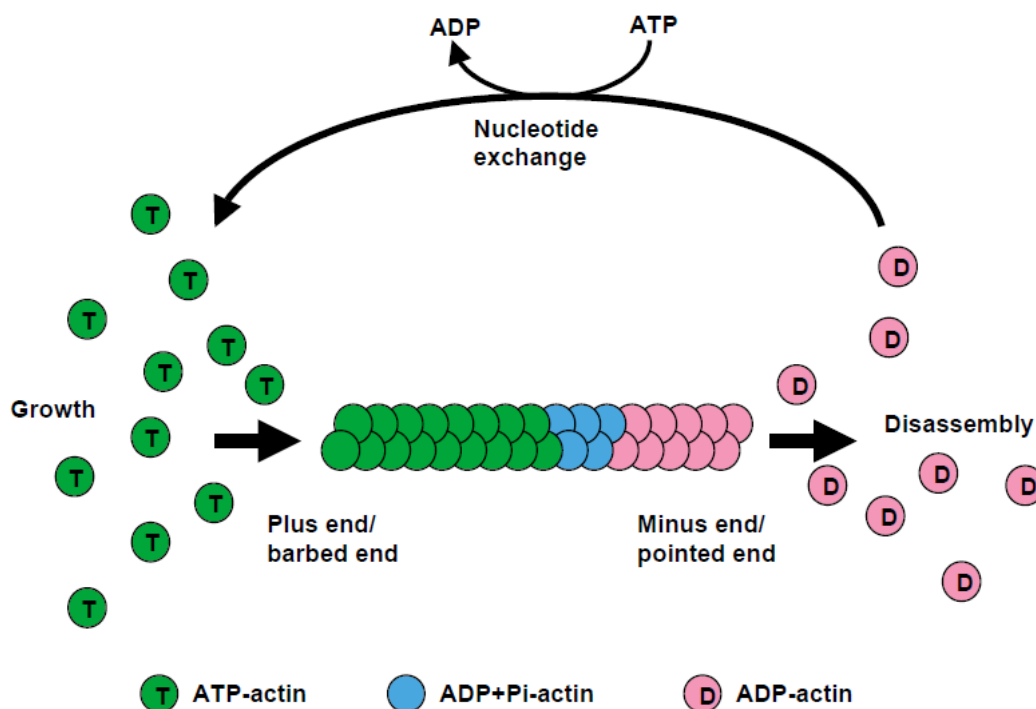
Figure 1.9: Actin polymerization and depolymerization, showing the different actin states. From Maiti and Bamburg (2004).

Actin filaments lack a clear striated organization in myoblasts, but as cells fuse to form myotubes, the actin filaments form aligned structures of uniform length and polarity (Ono, 2010), which is important for binding the force generating myosin motors in contracting muscle. Myosin structure can be divided in three domains: 1) the heavy chain or head domain, which

binds to actin and hydrolyses ATP; 2) the neck domain, which is an elongated α-helical region where light chains can bind and; 3) the tail domain, which is responsible for interactions with membranes, proteins or signalling molecules (Larson, 2004).

1.3.2.2 Microtubules

Microtubules are important to the cell because it can bind specific microtubule-proteins and motor proteins, giving rise to diverse functions such as cell movement, vesicle transport and chromosome segregation during mitosis (Downing and Nogales, 1998).

The microtubules in muscle cells are formed by the self-assembly of an α- and a β-tubulin subunit, giving rise to a heterodimer, called protofilament (Downing and Nogales, 1998). 12-15 parallel protofilaments, arranged head to tail, form a 25 nm hollow polymer (Figure 1.10) (Cheeseman and Desai, 2008). The α- and β-subunit are highly homogenous (≈ 63 %), and they both bind guanine nucleotides (Nogales, 2004). GTP bound to α tubulin is nonexchangeable, while GTP in β tubulin is exchangeable. Only tubulin dimers with GTP can polymerize, but this GTP is hydrolysed by interactions with the preceding tubulin dimer after addition to the microtubule, making the bound GDP nonexchangeable (Nogales, 2004). The microtubule is stabilized by an end layer of protofilaments still retaining their GTP. If the end layer is lost, either stochastically or by the action of external forces, the microtubule will rapidly depolymerize by releasing protofilaments, in a process known as a catastrophe. When the microtubule undergoes the reverse process, from depolymerisation to polymerization, it is known as a rescue. The catastrophe and rescue processes can coexist in the cell, giving a state of dynamic instability (Cheeseman and Desai, 2008). In addition to the inherent stability of the microtubule, the catastrophe/rescue ratio is modified by the interaction of cellular factors that either stabilize or destabilize the microtubule at different cell stages (Nogales, 2004).

Since the orientation of charged tubulin dimers are fixed, with α-subunits capping one end and β-subunits capping the other, the microtubule lattice has a polar charge, with a negative pole in the α-capped end and a positive pole in the β-capped end. This polarity is an important trait when moving particles *in vivo* (Cheeseman and Desai, 2008).
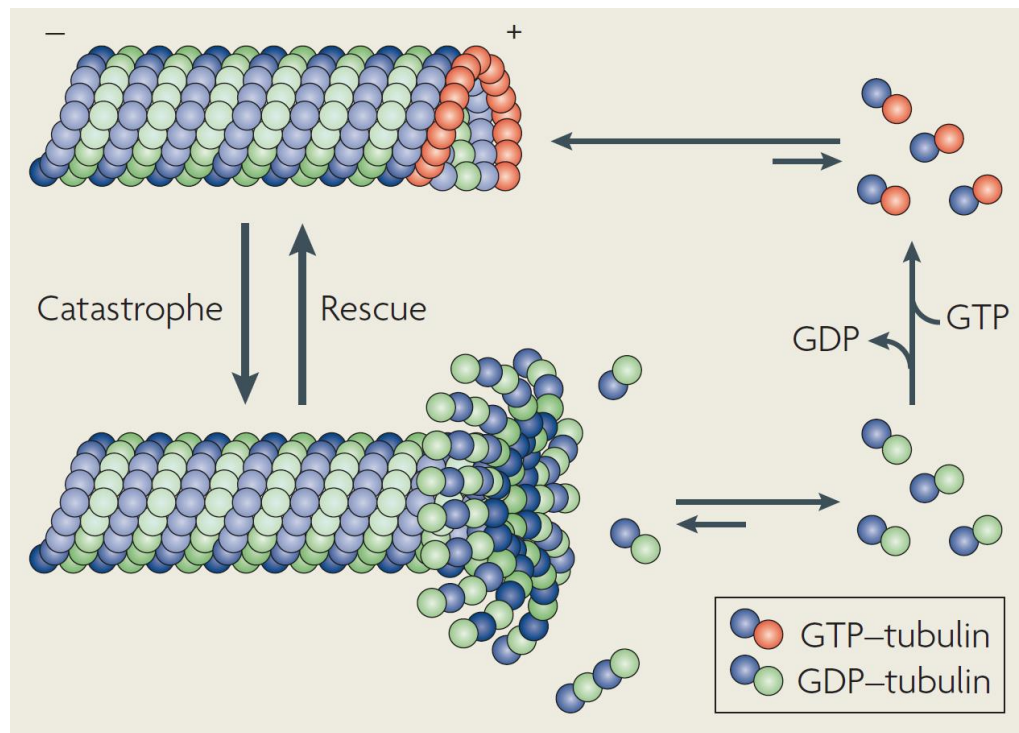
Figure 1.10: *Polymerization and depolymerisation of tubulin networks. From Cheeseman and Desai (2008).*

1.3.2.3 Intermediate filaments

Intermediate filament (IF) proteins, such as desmin, vimentin and nestin, reinforce the structures around myofibrillar Z-discs, they help connect the contractile apparatus with; subsarcolemmal cytoskeleton, the nucleus, and other cytoplasmic organelles (Carlsson and Thornell, 2001). Intermediate filaments are formed when eight rods of single filaments align with eight other rods, in a staggered array, and these filaments twist to create the final conformation of intermediate filaments (Figure 1.11) (Nature Education 2010). Desmin is the major muscle-specific IF protein, and is in fact the only IF protein in heart, skeletal and visceral smooth muscle (Small and Gimona, 1998). Desmin has a size of 53 kDa and is mainly located in the Z-disc of skeletal muscle (Paulin and Li, 2004). In skeletal muscles desmin appears in highest concentrations at attachment sites between myofibrils and tendons and at the chemical synapses between nerves and muscle fibres (Carlsson and Thornell, 2001). Defects in the desmin gene can lead to a loss of structural integrity and reduced functionality of muscle cells (Paulin and Li, 2004).
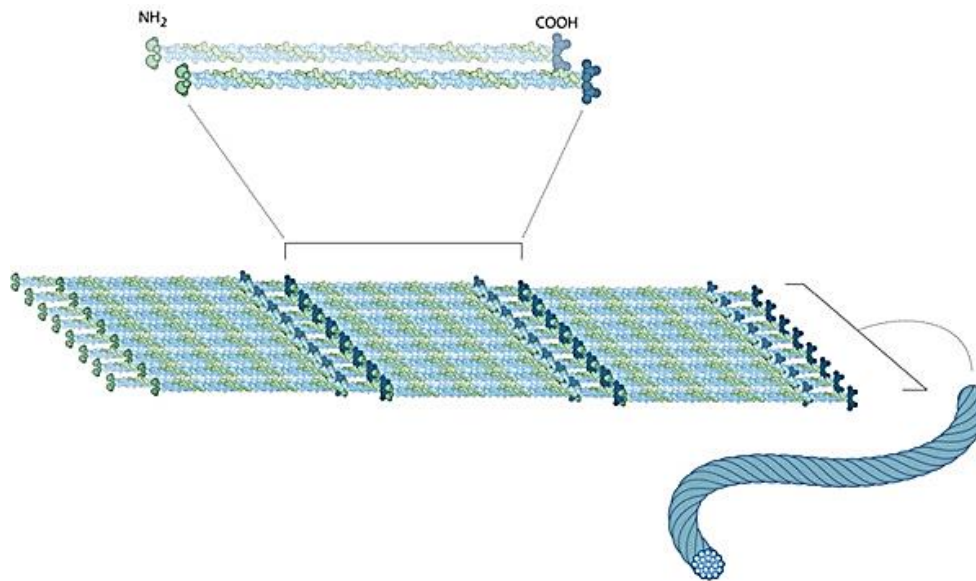
Figure 1.11: *Structure of intermediate filaments. From Nature Education (2010).*

1.3.3 The mitochondrion

Mitochondria are organelles within eukaryotic cells responsible for most of the energy production in the cell. The mitochondrion requires oxygen in the generation of ATP from fatty acids or sugars. They occupy about 25 % of the cytosolic volume and are among the largest organelles. The mitochondrion contains two membranes, where the outer membrane contains about 50 % lipid and 50 % proteins, while the inner contains about 20 % lipids and 80 % proteins. This configuration gives the membranes different permeability, where the inner membrane is much more rigid and less permeable than the outer. The outer membrane is smooth, while the inner membrane, where the final oxidation occurs, is infolded in cristae (Figure 1.12). It is also worth noting that mitochondria contain its own DNA, responsible for synthesis of specific proteins needed by the mitochondrion (Lodish et al., 1996).
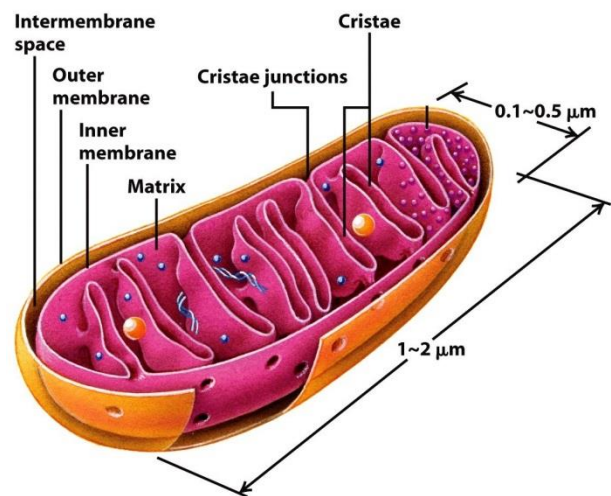
Figure 1.12: *Three dimensional diagram of a mitochondrion cut longitudinally. From Lodish et al. (2008).*

1.4 Aim of this study

Isolated satellite muscle cells can proliferate and differentiate *in vitro* if nutritional and environmental factors are adequate. One aim of this study is to characterise muscle cell proliferation and differentiation under normal *in vitro* conditions, to verify that protocols can be used in further experiments, and to give a better understanding of *in vitro* myogenesis in this specific cell system. Many methods of analysis will be the same as the ones planned to be used in later experiments, including real-time PCR, immunofluorescence analysis, western blotting and light microscopy, giving a good background representation of mechanisms controlling normal cell development and morphology in satellite muscle cell cultures.

Tenderness in the most important trait for purchase of meat cuts, and muscle cell death by apoptosis is proposed to play a role in the tenderisation process. One key feature after slaughter is that blood supply to muscles will cease, resulting in reduced nutrition and oxygen availability. The main aim of this study is to investigate how the descendants of satellite muscle cells react and adapt to removal of oxygen *in vitro,* to examine if these cells will initiate apoptosis. Assessment of apoptosis will be done by a wide range of analyses for different apoptotic markers, including mRNA expression of pro- and anti-apoptotic Bcl2-like proteins, analysis of mitochondrial changes by immunofluorescence and mRNA expression of mitochondrial apoptotic proteins, analyses of cytoskeleton re-organisation, and concentration changes of other protective proteins. This will hopefully further the understanding of muscle cell behaviour linked to post-mortem changes in the slaughtered animal.

2. Materials

2.1 Laboratory equipment and instruments

2.1.1 Laboratory equipment

Equipment	Supplier
6-, 24- and 96-well cell culture plates	Falcon
accu-jet pro pipette controller	BRAND
Cell scraper, 18 cm	BD Falcon
Countess® cell counting chamber slides	Invitrogen
Coverslip	Assistent
Eppendorf tubes	Eppendorf
Falcon tubes (15 ml, 50 ml)	VWR
Glass pasteur pipettes	VWR
Micro-homogenization tubes	Precellys 24
NuPAGE 10 % Bis-tris gels	Invitrogen
Nunclon Surface 25 cm^2 and 75 cm^2 cell growth flasks	Nunc
MicroAmp™ 96-well PCR plates	Applied Biosystems
Pipette tips	ART, BIOHIT and Thermo Scientific
Pipettes: Finnpipette	Thermo Scientific
Serological pipettes	VWR

2.1.2 Instruments

Instrument	Supplier
ABI Prism 7900HT Sequence detection system	Applied Biosystems
Axio Observer Z1 (microscope)	ZEISS
Biohazard safety cabinet class II	Scanlaf
Canon DS126271 (camera)	Canon
Countess, Automated Cell Counter	Invitrogen
Eppendorf Centrifuge 5430	Eppendorf
Ettan DIGE Imager	GE Healthcare
Galaxy 170S (Incubator)	New Brunswick
GeneAmp® PCR System 9700	Applied Biosystems
Glomax™ 96 microplate luminomenter	Promega
Heraeus Biofuge fresco (centrifuge)	Kendro
Leica DMIL LED, type: 11 090 137001 (light microscope)	Leica
Multifuge 3 S-R (centrifuge)	Kendro

2. Materials

NanoDrop$^{®}$ ND-1000 spectrophotometer	Thermo Scientific
PG5002-S DeltaRange$^{®}$ Balance	Mettler Toledo
Powerease™ 500 (gel electrophoresis apparatus)	Invitrogen
Power-pac™ HC (gel electrophoresis apparatus)	Bio-Rad
Precellys$^{®}$ 24 tissue homogenizer	Bertin Technologies
See saw rocker SSL4	Stuart$^{®}$
SUB Aqua 5 (heated water bath)	Grant
SW22 (heated water bath)	Julabo
C1301-230V (table top centrifuge)	Labnet International
Vacusafe (liquid disposal system)	Integra Biosciences

2.1.3 Software for data analysis

Software	Supplier
ImageQuant™ TL	GE Healthcare
Microsoft Office Excel 2010	Microsoft
SDS 2.2	Applied Biosystems
Zeiss Zen (blue edition)	Carl Zeiss Microscopy GmbH

2.2 Chemicals

Chemical	Supplier
AEBSF	Sigma-Aldrich
Dry milk powder	Unknown
Dulbecco's Phosphate-Buffered Saline, -CaCl$_2$, -MgCl$_2$	Life Technologies
ECL Cell attachment matrix	Millipore
ECL plex rainbow marker	GE Healthcare
Ethanol, C$_2$H$_5$OH	Kremetyl
Fluoromount-G™	Southern Biotech
JC-1 dye	Life technologies
Formaldehyde solution, 36.5-38 %	Sigma-Aldrich
Phosphatase buffer	Sigma-Aldrich
Triton X-100	Sigma-Aldrich
Trypan blue stain 0.4 %	Life technologies
0.05 % Trypsin-EDTA	Life technologies
Tween-20	Sigma-Aldrich

2.3 Medium

Medium	Components	Supplier
Proliferation medium (PM)	500 ml DMEM with GLUTAMAX-1 10 ml Fetal Bovine Serum 10 ml Ultroser™ G 2.5 ml Pen Strep 2.5 ml Fungizone®	Life technologies Life technologies Life sciences Life technologies Life technologies
Differentiation medium (DM)	500 ml DMEM with GLUTAMAX-1 10 ml Fetal Bovine Serum 2.5 ml Pen Strep 2.5 ml Fungizone® 25 pmol insulin from bovine pancreas	Life technologies Life technologies Life technologies Life technologies Sigma-Aldrich
Oxyrase stress medium	8.9 ml DM 1.0 ml 200 mM Sodium lactate 0.1 ml EC-Oxyrase®	 Oxyrase®, EC-0050

2.4 Primers and probes for real-time PCR

Primer/probe	Sequence
Aif (forward)	5'-GATCCTGATGTATGAAGAGAAAGCAA-3'
Aif (reverse)	5'-AATCAGGGCAACTCAGAGATAGCT-3'
Aif (probe)	5'-AGAAGCCAACAGGTCTCCCAGCCAA-3'
β-Actin (forward)	5'-CTGCGGCATTCACGAAACTA-3'
β-Actin (reverse)	5'-GCACCGTGTTGGCGTAGAG-3'
β-Actin (probe)	5'-ATTCCATCATGAAGTGTGACGTCGACATCC-3'
Bax (forward)	5'-TTTCTGACGGCAACTTCAACTG-3'
Bax (reverse)	5'-GGTGCACAGGGCCTTGAG-3'
Bax (probe)	5'-TTGTCGCCCTTTTCTACTTTGCCAGCA-3'
BCL2 (forward)	5'-GGAGCTGTATGGCCCTAGCA-3'
BCL2 (reverse)	5'-TGAGCAGTGCCTTCAGAGACA-3'
BCL2 (probe)	5'-CGGCCCCTGTTTGATTTCTCCTGG-3'
BID (forward)	5'-GCTTCGGCCACTGATCCA-3'
BID (reverse)	5'-CCCCGGGCTTTAAAATGGT-3'
BID (probe)	5'-CCCAAGACGATCACGGAGTGCCA-3'
Bim (forward)	5'-GCCCGGCACCCATGA-3'
Bim (reverse)	5'-TTGAAGGCCTGGCAAGGA-3'
Bim (probe)	5'-TGTGACAAATCCACACAGACCCCAAGC-3'

2. Materials

Desmin (forward)	5'-GCTGAAAGAAGAAGCGGAGAAC-3'
Desmin (reverse)	5'-GAGCTAGAGTGGCTGCATCCA-3'
Desmin (probe)	5'-ATTTGGCTGCCTTCCGAGCCG-3'
MHC (forward)	5'-CTCACCCTGAAATGGGAACCT-3'
MHC (reverse)	5'-GGAGAACCAGGCCAACAATG-3'
MHC (probe)	5'-TCAGCCCTCCTTCCTCACCATGGG-3'
MyoD (forward)	5'-CCCAAAGATTGCGCTTAAGTG-3'
MyoD (reverse)	5'-AGTTCCTTCGCCTCTCCTACCT-3'
MyoD (probe)	5'-ACCACTCTCCTCCCAACAGCGCTTTAAA-3'
Myogenin (forward)	5'-CCCTACAGACGCCCACAATC-3'
Myogenin (reverse)	5'-AGCGACATCCTCCACTGTGAT-3'
Myogenin (probe)	5'-CACTCCCTCACCTCCATCGTGGACA-3'
TATA (forward)	5'-CGTTTTGCTGCTGTAATCATGAG-3'
TATA (reverse)	5'-CCATCTTCCCAGAACTGAATATCA-3'
TATA (probe)	5'-ATAAGAGAGCCCCGCACCACTGCA-3'

2.5 Antibodies for western blot

Antibody	Supplier	Product number
α-tubulin	Sigma-Aldrich	T5168
Actin	Abcam	ab1801
CY3	GE Healthcare	PA43010V
CY5	GE Healthcare	PA45012V
Desmin	Abcam	Ab8592
Hsp70	Abcam	ab13529-50
MyoD	Santa Cruz Bio	Sc-304
PARK7	Abcam	ab37180-100

2.6 Antibodies specifically for immunofluorescence

Antibody	Supplier	Product number
Alexa-488 Phalloidin	Molecular probes, Invitrogen	A12379
Alexa-546	Invitrogen	A11030
DAPI	Molecular probes, Invitrogen	D1306
Hoechst	Santa Cruz Biotechnology	sc-200908

2.7 Kit

Kit	Contents	Supplier
Caspase-Glo® 3/7 Assay	Caspase-Glo® 3/7 Buffer Caspase-Glo® 3/7 Substrate	Promega Corporation
Caspase-Glo® 9 Assay	Caspase-Glo® 9 Buffer Caspase-Glo® 9 Substrate	Promega Corporation
CellTiter-Glo® Luminescent Cell Viability Assay	CellTiter-Glo® Buffer CellTiter-Glo® Substrate	Promega Corporation
iBlot® Dry Blotting System	Complete transfer stack, including anode, nitrocellulose membrane, cathode, filter paper and sponge.	Invitrogen™
RNeasy® Mini Kit (50)	RNeasy Mini Spin Columns (pink) Collection Tubes (1.5 ml) Collection Tubes (2 ml) Buffer RLT 45 ml Buffer RW1 45 ml Buffer RPE (concentrate) 11 ml RNase-Free Water 10 ml	QIAGEN®
TaqMan® 1000 Rxn PCR Core Reagents	AmpliTaq Gold® DNA Polymerase AmpErase® UNG dUTP dATP dCTP dGTP TaqMan® Buffer A 25 mM $MgCl_2$ Solution	Applied Biosystems®
TaqMan® Reverse Transcription Reagents	MultiScribe™ Reverse Transcriptase RNase Inhibitor dNTP Mixture Oligo d(T)16 Random hexamers 10X RT Buffer Magnesium chloride solution	Applied Biosystems®
Western blot sample preparation	NuPAGE® MOPS SDS Running Buffer (NP0001) NuPAGE® Antioxidant (NP0005) NuPAGE® LDS Sample Buffer (NP0007) NuPAGE® Sample Reducing Agent (NP0009)	Life technologies

2. Materials

2.8 Buffers and solutions

Buffer/Solution	Components
Lysis buffer	2ml 0,5 M Tris, pH 6.8
	1 ml 0,5 M EDTA
	0.21 g NaF
	1.34 g Na-pyrophosphate
	20 ml 10 % SDS
	77 mldH$_2$O
Added immediately before use:	1 ml 100 mM Na-orto Vanadate
	1 ml 100 mM Phenylmethanesulfonyl fluoride
PBS-T (0.01 %)	PBS
	100 µl Tween 20
	995.1 ml dH$_2$O
Sørensen-buffer (pH 7.4)	11.5 g 0.2 M Na$_2$HPO$_4$ (dibasic)
	2.96 g 0.2 M Na$_2$HPO$_4$ (monobasic)
	500 ml dH$_2$O
TBS-t (pH 7.4)	1.21 g Tris
	8.0 g NaCl
	3.8 ml 1M HCl
	1 ml Tween 20
	995.2 ml dH$_2$O

3. Methods

3.1 Bovine skeletal muscle progenitor cells as a model system

Satellite cell populations are isolated through enzymatic digestion of skeletal muscles, and satellite cells are considered the major source of myogenic progenitor cells in adult muscle (Danoviz and Yablonka-Reuveni, 2012). This means that all cells from one batch of isolation have the same genetic material as the animal it derived from. If the number of myoblast passages is kept low when growing cells, they will probably keep many of their innate signaling pathways (Yablonka-Reuveni and Day, 2011). On the other hand, if satellite progenitor cells are passaged long-term as myoblasts (e.g. in myogenic cell lines), it can lead to major variations in regulatory feedback and these cells might not reflect the features of the ancestor cells(Yablonka-Reuveni and Day, 2011).

3.1.1 Coating flasks, plates and microscopy dishes

Extracellular matrix (ECM) is a non-cellular component present in all tissue *in vivo*. ECM is essential for physical scaffolding for cellular constituents and is fundamental for initiation of biochemical and biomechanical cues required for tissue morphogenesis and differentiation (Frantz et al., 2010). The ECM contains various proteins and polysaccharides, which is highly specific for each tissue (Frantz et al., 2010). To effectively grow muscle cells *in vitro*, the cells need to be introduced to an environment similar to the one *in vivo*. ECL can be used as a surfactant to mimic characteristics of ECM found in muscle tissue. ECL is shown to give muscle progenitor cells good conditions to proliferate and differentiate, without cells loosening from the coated surface under normal growth conditions (Boonen et al., 2009).

Method:

- ECL was directly dispersed on the bottom with a cell scraper for flasks, while ECL was mixed with PM when coating plates and dishes.

- Volume of ECL and PM, and the surface area of each plate, dish and flask is shown in table 3.1.

- When 24 well plates were used for microscopy analysis, they were inlaid with a coverslip. The coverslip was placed in the well and washed with ethanol and air dried, before adding ECL and PM to the well.

- The coated flask, plate or dish was incubated on a LAF bench for 2-4h.

- Medium was subsequently removed from plates and dishes.

3. Methods

- Finally the plates, dishes or flasks were washed three times with PBS and stored at 4 °C.

Table 3.1: *Volumes of ECL and PM for coating of flasks and plates.*

Values are given for each well.

Plate/flask	ECL (µl)	Proliferation medium (ml)	Surface area (cm^2)
Big flask	150	-	75
Small flask	50	-	25
6 well plate	30	4	10
24 well plate	6	0.5	2.0
96 well plate	0.9	0.1	0.32
Microscopy dish	30	2	12.25

3.1.2 Thawing and growing cells

Primary satellite muscle cells from bovine *longissimus thoracis* (sirloin) were used in all experiments (Rønning et al., 2013). The cells were already isolated and stored in liquid nitrogen in aliquots of 1 ml, containing primary bovine cells, 20% DMSO and FBS. Contents of proliferation medium (PM) and differentiation medium (DM) is presented in section 2.3. DMEM was used as a basal medium for growth, FBS contains a wide array of proteins which are essential for the cells to grow and proliferate, Pen Strep is an antibiotic mixture to keep unwanted bacteria from growing in the medium and Fungizone is used to inhibit growth of yeast and fungi in the medium. Ultroser™ G can be used as a substitute for FBS, and will further facilitate proliferation of muscle cells. DM contained the peptide hormone insulin, which is shown to be crucial for a timely differentiation (Bateman and McNeill, 2004). DM had a lower serum concentration, thus starving the cells, inducing rapid differentiation (Yablonka-Reuveni and Day, 2011).

Method:

- The sample tube with isolated satellite cells was thawed in a water bath at 37 °C until all the ice was liquefied.

- The sample was then rapidly transferred to a 15 ml falcon tube, re-suspended in 5 ml PM before centrifugation at 550 rpm for 6 min.

- The supernatant was removed and the cell pellet re-suspended in PM. The amount of PM in this step depended on the size of flask used, where 5 ml was used for 25 cm^2 flasks and 15 ml was used for 75 cm^2 flasks.

- The cells were transferred to the pre-coated flask and incubated at 37 °C and 5 % CO_2.

- The medium was changed every 2-3 days thereafter, until the cells were harvested for experiments or split for further proliferation.

3.1.3 Splitting cells

Trypsin was used to loosen the cells from the ECL coating. This proteolytic enzyme is known as a serine protease, cleaving polypeptide chains at positively charged arginine or lysine residues (Di Cera, 2009).This procedure was carried out if a higher number of cells were desired for experiments. The time of splitting was determined by the density of cells in the flask, and could vary from one day up to five days. Splitting was done either by transferring the cells from one 25 cm^2 flask to one 75 cm^2 flask or from one 75 cm^2 flask to two 75 cm^2 flasks.

Method:
- PM was removed from the flask and the cells were washed three times with PBS (4 ml for 75 cm^2 flasks and 2 ml for 25 cm^2 flasks).

- Trypsin was added to the flask (3 ml for 75 cm^2 flasks and 1.5 ml for 25 cm^2 flasks) and then incubated at 37 °C for 4-5 min, or until the cells had detached from the surface.

- The flask was examined with light microscope to see if the cells had loosened from the coating, if not, they would be incubated for a longer period.

- When the cells had detached, 5 ml PM was added and repeatedly washed over the surface where cells had grown.

- The suspension was transferred to a 15 ml Falcon tube and the rest of this procedure was carried out as described in 3.1.2 from the centrifugation step and out.

3.1.4 Seeding cells for experiments and cell counting
Method:
- The cells from proliferation flasks were treated with trypsin as in step 3.1.3.

- After centrifugation and re-suspension steps the number of cells was counted using a Countess® automated cell counter.

- This was done by mixing 10 µl of the re-suspended sample and 10 µl Trypan blue stain (0.4 %) in an eppendorf tube.

3. Methods

- 10 µl of this mixture was loaded on a cell counting chamber slide, placed in the cell counter and counted automatically.

- The results were checked manually to verify that the counter included the desired cells. If not, the apparatus was calibrated and sample re-counted.

- The cells were then seeded on pre-coated plates or dishes, and PM was added.

- 6 well plates were used for real-time PCR and western blot analyses. 24 well plates, with coverslips, and microscopy slides were used for immunofluorescence analyses. 96 well plates were used for casapase 3/7, caspase 9 and viability assays.

- Approximate number of cells seeded and the volume of PM in each well for different plates are shown in table 3.2. The cells were incubated at 37 °C and 5 % CO_2 for all the experiments.

Table 3.2: Overview of approximate cell distribution for experiments.

Plate	Number of cells in each well	Proliferation medium in each well (ml)
96 well plate	3000	0.1
24 well plate	12500	0.5
Microscopy dish	20000	2
6 well plate	50000	4

3.1.5 Proliferation and differentiation experiments

Method:

- Proliferating cells were grown in PM for 2d.

- Differentiated samples were grown in PM for 2 days, and then the cells were induced to differentiation by adding DM for 2d, 4d, or 6d.

- Independent of treatment, the medium was changed every 2-3 days. This was done by removing the old medium and replacing it with the appropriate medium, which was heated to 37 °C in a water bath beforehand.

- Cells from these experiments were analyzed by real-time PCR, western blot, light microscopy and immunofluorescence microscopy.

3.2 Stress experiments

EC-Oxyrase® was used in experiments where removal of available oxygen was desired. EC-Oxyrase® is an enzyme system that depletes the medium of oxygen when a substrate, such as sodium lactate, is available. The enzyme is derived from the cytoplasmic membrane of *Escherichia coli,* and contains a buffered suspension of particles no larger than 0.2 microns (Oxyrase, Inc., 2011). Removal of oxygen was done to mimic some of the changes in extracellular conditions for muscle cells post-slaughter, to investigate if muscle cells show signs of cellular death by apoptosis. To best represent muscle cells *in vivo*, the cells were grown to differentiation before oxygen removal.

Method:

- The control for stress experiments was not treated with EC-Oxyrase®.

- Anaerobic medium contained 89.1 % DM, 9.9 % sodium lactate and 1 % EC-Oxyrase®.

- Stress samples were incubated at 37°C/5% CO2for 15 min., 30 min., 45 min., 60 min., 2 h., 4 h., 6 h. or 22 h.

- Cells from these experiments were analyzed by real-time PCR, western blot, light microscopy, live and fixed immunofluorescence microscopy, and caspase 3/7-, caspase 9- and viability-assays.

3.3 Microscopy

3.3.1 Light microscopy

The light microscopy was done to follow the day-to-day development of cells, helping to make the decisions of when to introduce the cells to new medium, when to split the cells or when to harvest the cells. In addition microscopy pictures were taken to illustrate the development of cells under proliferation, differentiation or after removal of oxygen. Microscopy was performed on a Leica DMIL LED microscope and pictures were taken with a Canon DS126271 camera. The general procedure for taking pictures was to get an overview of all samples and choosing representative areas for each test parameter. All pictures were taken at $10\times$ magnification.

3.3.2 Immunofluorescence microscopy on fixed samples

Immunofluorescence microscopy makes use of fluorescent chemicals in conjunction with specific antibodies for a desired protein. The fluorescent chemical can be directly coupled to the primary antibody or to a secondary antibody, which in turn interacts with the specific primary

antibody. Fluorescent chemicals absorb light at one wavelength and emit light at a longer wavelength. All other light than the emitted is filtered out in a dichromatic filter and a barrier filter, to ensure detection of emitted light only (Lodish et al., 1996).

3.3.2.1 Fixation

Fixation was performed to denature most proteins and nucleic acids in the sample. The formaldehyde treatment stabilizes protein-protein and protein-nucleic acid interactions by cross-linking amino groups on adjacent molecules. This results in stable molecules for further procedures (Lodish et al., 1996).

Method:

- The original growth medium was removed and cells were washed with PBS once.

- The sample was then incubated with cold 2 % PFA, diluted in Sørensen buffer, for 20 min. in a fume cupboard.

- The sample was washed three times with PBS for 5 min.

3.3.2.2 Permeabilization

Permeability is the measure of the ability of membrane to allow molecules to pass through. By increasing the permeability, with the use of detergents, larger and more complex molecules, such as antibody complexes, can pass through the membrane.

Method:

- Sample was incubated on the lab bench with 0.1 % Triton X-100, diluted in PBS, for 10 min.

- The sample was washed once with PBS.

3.3.2.3 Immunologic detection

Blocking was performed to avoid non-specific adsorption of antibodies. Antibody interaction and characteristics is described in section 3.5. Antibodies used in the procedure are listed in section 2.6. The procedure was performed on coverslip or in a microscopy dish.

<u>Coverslip procedure</u>

Method:

- The coverslip was taken out of the well and inverted in 35 µl blocking solution containing 5 % dry milk, diluted in PBS-T, and incubated for 30 min. on the lab bench.

- The coverslip was moved to a new location containing 35 µl primary antibodies, diluted in 2 % dry milk in PBS-T, and incubated on the lab bench for at least one h.

- The coverslip was washed on a drop of PBS-T for 10 min. three times.

- The coverslip was moved onto a new 35 µl drop, containing secondary antibodies diluted in 2 % dry milk in PBS-T, and incubated on the lab bench at least 30 min. covered by aluminium foil.

- The coverslip was once again washed three times with PBS-T for 10 min.

Microscopy dish procedure

Method:

- All blocking, staining and washing took place in the dish. The procedure was the same as for coverslips, but 100 µl solutions were used in each step containing antibodies.

- Wash procedures was carried out using about 500 µl PBS-T each time.

3.3.2.4 Mounting of coverslips

This protocol was only carried out for coverslip procedures.

Method:

- 5 µl mounting medium was placed on a microscopy object glass.

- The coverslip was placed directly on the medium and lightly pressed down against the object glass until air bubbles was removed.

- The finished sample was laid in the dark to dry before fluorescence microscopy analysis.

3.3.2.5 Microscopy analysis

A ZEISS Axio Observer Z1 microscope was used for all microscopy analysis. All samples were examined under the microscope and representative pictures from each experiment/sample were taken.

3.3.3 Live fluorescence microscopy

Live microscopy implies that the same cell sample was analysed before and after removal of oxygen. This gave an opportunity to investigate responses to removal of oxygen without the use of any destructive treatments, e.g. denaturing or lysing agents. Live cell analysis are on the other hand restricted to methods that leave the cells intact, and this limits the extent of analyses available for live cell experiments. JC-1 is a membrane-permeant dye containing positively charged probes that can transverse both the cytoplasmic membrane and the mitochondrial membrane, and subsequently accumulate in the mitochondrion of live cells (Smiley et al., 1991). Since the probe is positively charged it accumulates at the negatively charged inside of the

mitochondrial membrane, where the probes create fluorescent red aggregates within the mitochondrial intermembrane space. If the membrane potential decreases, some of the probes disassociate from the membrane and monomers of JC-1 dye is formed, resulting in a green fluorescent emission (Di Lisa et al., 1995). Cells grown on a microscopy dish with glass bottom was used in these experiments.

Method:

- Growth medium was removed and 2 ml DM containing 4 µl JC-1 dye and 4 µl Hoechst dye was added to the dish.

- The microscopy dish was incubated at 37 °C for 10 min.

- Medium was removed and the dish was washed with PBS twice.

- Pictures were taken as controls.

- 1 ml oxyrase stress medium was added to the dish.

- The microscopy dish was incubated at 37 °C until pictures were taken, and subsequently returned to the incubator.

- Pictures were taken at 15 min., 30 min., 45 min., 60 min., 2 h., 4 h., 6 h. and overnight.

- Pictures were analysed by calculating areas of green and red emission, as well as their intensity, using ZEISS ZEN software.

3.4 Quantification of mRNA

Real-time PCR was used to quantify relative mRNA expression. Polymerase chain reaction (PCR) is a method to copy specific DNA sequences *in vitro.* The amplification of target DNA from the entire template is done in sequences of heating and cooling, to allow template, primers and polymerase to re-anneal and copy DNA many times. The accumulation of DNA is monitored during real-time PCR, by detecting the total fluorescence from probes that emits a fluorescent signal upon binding to DNA. This gives a rise in fluorescence that is proportional with the amount of DNA amplified. Real-time PCR also gives the opportunity to quantify amounts of target DNA and relative concentrations of mRNA in different samples (Madigan et al., 2009). Only specific probes were used in these analyses.

3.4.1. Lysing cells

Lysing agent contained a highly denaturing guanidine-thiocynate buffer, which immediately inactivates RNases to ensure minimal degradation of RNA from the sample (QIAGEN, 2006).

Materials:

- RNeasy® Mini Kit (50)

Method:

- Medium was removed from the wells and they were washed twice with PBS.

- 350 µl RLT buffer was added to each well and the cells were scraped off using a cell scraper.

- Cells were transferred to a micro homogenization tube and the sample was homogenized in in a rotor stator homogenizer for 30 sec. at 6000 rpm.

- The homogenized sample was stored in an autoclaved eppendorf tube at -80 °C until RNA isolation.

3.4.2 Isolation of RNA

Isolation of RNA with this procedure implies removal of all other components from the lysed cells, except of RNA larger than 200 bases. This is accomplished by addition of ethanol, to provide appropriate binding conditions, and subsequent centrifugation in a spin column with a specialized membrane. The membrane binds RNA specifically, while other contaminants are washed away in a number of washing procedures (QIAGEN, 2006)

Materials:

- RNeasy® Mini Kit (50)

Method:

- Sample was thawed on ice.

- 350 µl 70 % ethanol was added to the thawed homogenized sample, and subsequently mixed with a pipette.

- The entire volume was transferred to an RNeasy spin column placed in a 2 ml collection tube. This was centrifuged for 15 sec. at 10000 rpm and the flow-through was discarded.

- 350 µl RW1 buffer from the kit was added to the spin column and centrifuged once again for 15 sec. at 10000 rpm. The flow-through was discarded.

- 80 µl DNase mix was added directly to the membrane of the spin column and this was incubated in room temperature for 15 min.

- After the incubation 350 µl RW1 buffer from the kit was once again added to the spin column and centrifuged for 15 sec. at 10000 rpm. The flow-through was discarded.

- 500 µl RPE buffer from the kit was added to the spin column and centrifuged for 2 min. at 10000 rpm. The flow-through was discarded and this step was done once more, but with 1 min. centrifugation.

- The spin column was placed in a 1.5 ml eppendorf tube and 30 µl RNase-free water was placed directly on the membrane. This was centrifuged for 1 min. at 10000 rpm and the flow-through was placed on the membrane again. This was then centrifuged one last time for 1 min. at 10000 rpm.

- The RNA yield was measured on Nano-drop. RNase-free water was used as a blank sample in the Nano-drop procedure, and 1.5 µl was used as sample size.

- The isolated RNA was stored at -80 °C.

3.4.3 Making cDNA

cDNA is the complementary DNA from a RNA template. The retrovirus enzyme reverse transcriptase is a DNA polymerase that uses DNA or RNA as template to create double stranded DNA helices. Double-stranded DNA is needed to perform the real-time PCR procedure, and it has the added benefit of being more stable than RNA single-strands. Using cDNA from RNA transcripts ensures that the investigated genes were expressed under experimental conditions, and not that the results came from innate DNA of the cells. The isolated RNA from section 3.4.2 was used as template to create cDNA for further use in real-time PCR (Alberts et al., 1989).

Materials:

- TaqMan® Reverse Transcription Reagents.

Method:

- A master mix with all the reagents for cDNA synthesis was made, as shown in table 3.3.

Table3.3: Master mix used in cDNA synthesis of one sample.

Reagent	Volume (µl)
10x RT buffer	2
25 mM MgCl2	4.4
Deoxy NTPs	4
oligodT	1
RNaseinhibitor	0.4
MultiScribe Reverse Transcriptase	0.5
Total volume	12.3

- The reagents were added to an eppendorf tube and mixed with a pipette before transferring it to a cDNA reaction tube.

- A mixture of deionized water and RNA from step 3.4.2 was added to the cDNA reaction tube, where the amount of each was calculated on the basis of Nano-drop measurements, with a total volume of 7.7 µl.

- The aim was for the sample to contain 400 ng RNA, if this could not be attained 7.7 µl of RNA isolate was added and no water.

- All work was done while the RNA samples and master mix were kept on ice.

- The prepared sample was placed in a GeneAmp PCR apparatus and heated with the following procedure: 48 °C for 30 min. and 95 °C for 5 min.

- The sample was stored at -80 °C or used immediately in real-time PCR analysis. Before use in the real-time PCR procedure the cDNA samples were diluted by adding 110 µl dH$_2$O.

3.4.4 Real-time PCR

Materials:

- TaqMan® 1000 Rxn PCR Core Reagents.

Method:

- All master mixes and cDNA samples were kept on ice until centrifugation of the 96 well PCR plates.

3. Methods

- The procedure starts with the making of master mixes for the real-time PCR reactions. The master mixes contained reagents as shown in table 3.4, where the probe and primers were specific for each target gene, as shown in section 2.4.

- The reagents were added to an eppendorf tube in the order presented in table 3.4, where all reagents except dH_2O, UNG and polymerase were vortex mixed before addition to the master mix.

Table 3.4: Master mix for one real-time PCR sample.

Reagent	Volume (µl)
dH_2O	9.65
TaqMan® Buffer A	2.5
MgCl2	5
dATP	0.5
dUTP	0.5
dGTP	0.5
dCTP	0.5
Reverse primer	0.5
Forward primer	0.5
Probe	0.5
AmpErase® UNG	0.1
AmpliTaq Gold® DNA Polymerase	0.25
Total volume	21

- The master mix for each gene was centrifuged with a tabletop centrifuge, mixed with a pipette and distributed on 96-well PCR plates in triplicates for each cDNA sample to be analyzed.

- 21 µl of the appropriate master mix was loaded in each corresponding well on the 96 well PCR plate and then 4 µl of diluted cDNA was added to the wells.

- After all the samples were loaded the plate was covered with a plastic film and centrifuged for 2 min. at 2500 rpm.

- The side with plastic film was covered with a rubber mat and the plate was placed in the real-time PCR apparatus (Applied Biosystems 7900HT Sequence Detection System).

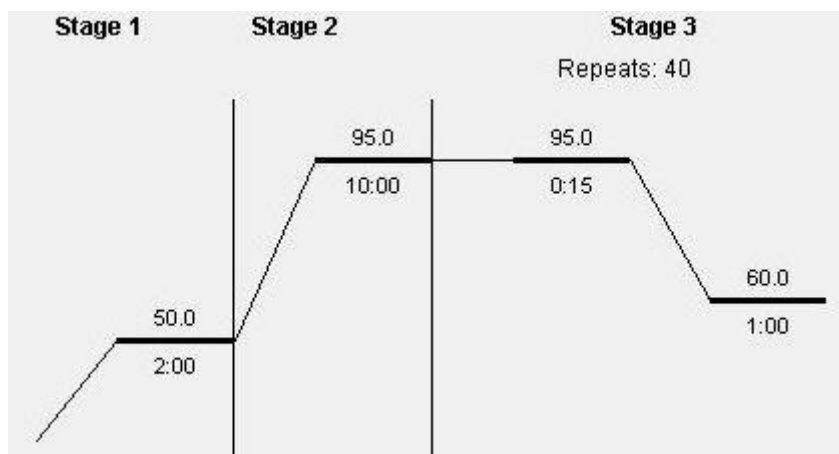- The real-time PCR thermal profile was as shown in figure 3.1, where data was collected only during stage 3.

Figure 3.1: *Thermal profile of real-time PCR*

3.4.5 Calculation of relative mRNA expression

The procedure for calculating relative gene expressions was modified from Livak and Schmittgen (2001). β-actin was used as internal control in preliminary experiments, while samples only incubated in PM was used as calibrator. TATA was used as internal control in stress experiments, while samples without removal of oxygen were used as calibrator. Information about experimental conditions for each analysis can be found in section 4.1.4 and 4.2.3.

Method:

- C_T values were exported from the SDS 2.2 program to Microsoft Excel 2010.

- Average C_T value of technical triplicates for each sample was calculated.

- Average internal control C_T value was subtracted from the average C_T value for each examined gene, giving the ΔC_T value.

- Average value of calibrator samples for each gene was calculated within one experiment.

- The average value of calibrator samples were used to calculate relative expression, giving the $\Delta\Delta C_T$ value.

- Fold difference (FD) was calculated using the following equation: $FD = 2^{-\Delta\Delta C_T}$.

- Statistical analyses were carried out as paired Student's t-test in Microsoft Excel, where experimental conditions were compared to the calibrator, using two-tailed distribution and assumption of equal variance.

3.5 Western blot

Western blot is a method which utilizes the specificity of antibodies to detect proteins in samples (Copeland, 1994). An antibody is only able to bind to one specific molecule and can therefore be used to confirm the identity of a protein or it can be used to screen samples for a specific protein (Copeland, 1994). In the western blot procedure the first step is to lyse cells to be able to separate proteins by gel electrophoresis. Following electrophoresis the proteins will be separated in different regions of the gel, due to the proteins different size, shape or charge (Bollag and Edelstein, 1991). These proteins are transferred to a nitrocellulose membrane by another electrophoretic process, called blotting, retaining their individual relative position from the gel (Copeland, 1994). The rest of the nitrocellulose membrane is coated with non-antigenic protein to avoid non-specific binding of antibodies, in a process named blocking (Copeland, 1994). The membrane is then stained with primary antibody against the target protein (Copeland, 1994), including an antibody for a reference protein if quantification is the aim of the experiment. If the target protein(s) is on the sheet the antibodies will attach themselves on the protein surface (Copeland, 1994). A secondary antibody with specificity for the primary antibody is then added, and this will attach to the primary antibody, giving an antibody-antibody-protein complex fixated on the nitrocellulose membrane (Bollag and Edelstein, 1991). It's important to note that the primary and secondary antibodies need to be prepared from different species, the main reason being that antibodies from different species will give a specific cross-reaction between the two classes of antibodies (Copeland, 1994). The secondary antibody is usually conjugated to a labeling agent (Bollag and Edelstein, 1991), such as a fluorescent molecule, which can be identified in a fluorescence detecting instrument.

3.5.1 Protein isolation

Cells were lysed to degrade cell membranes, giving a release of proteins and other intracellular components to the solution. AEBSF and phosphatase buffer prevent the cells own enzymes from degrading proteins in the sample. SDS is an anionic detergent, and is used in the lysis buffer to denature proteins and give them a universal negative charge. The procedure explains volumes used for cells seeded in one well on a 6 well plate.

Method:
- Medium was removed from the cultured cells and they were washed twice in PBS.

- A lysis mixture containing lysis buffer, phosphatase buffer and AEBSF was prepared, where the ratio of reagents was 1000:10:5 respectively.

3. Methods

- The cells were lysed in 150 µl lysis mixture for 10 minutes on ice and subsequently transferred to an eppendorf tube.

- The lysed cells were then stored at -20 °C.

3.5.2 Gel electrophoresis

Centrifugation was done to separate proteins from other unwanted cell components. Heating of the sample ensured better binding of SDS to the proteins and promotes denaturing of proteins. This procedure explains the making of one sample for one well on a gel in the sample preparation part, while the procedure for the gel electrophoresis apparatus includes a full setup that can hold two gels.

Method:

Sample preparation:

- Sample was thawed in room temperature.

- Before gel electrophoresis the sample was centrifuged at 10 000 g for 10 minutes.

- 6.5 µl of the supernatant was transferred to a new eppendorf tube and mixed with 2,5 µl NuPAGE® LDS Sample Buffer (4X) and 1 µl NuPAGE® reducing agent (10X).

- The eppendorf tube was then heated at 70 °C for 10 minutes.

Gel electrophoresis:

- Running buffers was prepared by adding 50 ml NuPAGE® MOPS SDS running buffer to 950 ml dH$_2$O. 200 ml of running buffer was mixed with 500 µl NuPAGE® Antioxidant.

- The gel electrophoresis apparatus was assembled and the gel (NuPage® 10 % Bis-Tris by Novex®) was put in its appropriate chamber.

- The inner chamber was filled with running buffer containing antioxidant and the outer chamber with running buffer without antioxidants.

- 10 µl of sample was then loaded in a predetermined pattern in the wells on the gel.

- The first well for each different antibody procedure was loaded with 1.5 µl ECL* plex rainbow marker, used as a marker for protein sizes in the gel.

- The electrophoresis was run at 200 V for about 1 hour, until the smallest proteins in the ladder reached the bottom of the gel.

* NB! Not to be confused with ECL coating reagent

3.5.3 Blotting

Blotting was performed using iBlot® Dry Blotting System (Invitrogen™).

Method:

- The device was prepared by placing an Anode Stack, with an attached nitrocellulose membrane, on the blotting surface.

- The pre-run gel was then placed on the Anode Stack and an iBlot® filter paper, soaked in deionized water, was placed on top of the gel.

- Any air bubbles were removed with a Blotting Roller.

- The Cathode Stack was placed on top and once again removed air bubbles with the Blotting Roller.

- A Disposable Sponge was placed in the top tray, the device was closed and the blotting procedure started.

- The blotting program was run for 6 minutes, and afterwards everything but the nitrocellulose membrane was discarded.

3.5.4 Staining of membranes

Overview of antibodies used can be found in section 2.5.

Method:

- The nitrocellulose membrane was incubated in a blocking solution (2 % ECL* Advance™ blocking agent diluted in TBS-T) for 1 hour with continually shaking at 30 tilts each minute.

- The primary antibody was made by mixing a blocking solution (0.5 % ECL* Advance® blocking agent diluted in TBS-T) and primary antibodies.

- The blocking solution was discarded and the membrane was incubated with the primary antibodies for 1 hour while shaking and subsequently stored at 4 °C over night.

- The next morning the membrane was washed 3 times for 10 minutes with TBS-T while shaking.

- The secondary antibody mixture was made by mixing TBS-T containing 0.5 % ECL Advance® blocking agent and secondary antibodies.

* NB! Not to be confused with ECL coating reagent

- The membrane was incubated with secondary antibodies for 1 hour with shaking.

- The membrane was washed 3 times for 5 minutes with TBS-T while shaking.

- The membrane was dried on filter paper until it was completely dry.

- During this entire procedure the tray with the nitrocellulose membrane was covered by aluminum foil.

- All volumes of blocking agent, antibodies and washing were such that the entire membrane was covered in solution.

- The dried membrane was scanned on an Ettan DIGE Imager (GE Healthcare).

3.5.5 Quantification of blots

The software is used to quantify the amount of protein in each sample by using the image from the scanning process. Then the amount of the reference protein from each experimental condition was used as a standard to give the normalized value of the desired protein in each sample. ImageQuant™ TL software (GE Healthcare) was used in this procedure.

Method:

- Relative protein concentration was calculated by the following equation: $N = \frac{S}{R}$, where N was the calculated normalized value, and R is the amount of reference protein and S is the amount of the specific desired protein from blots in ImageQuant™.

- The normalized values were then compared to show differences between the different conditions.

- Statistical analyses were carried out as paired Student's t-test between experimental variables, using two-tailed distribution and assumption of equal variance.

3.6 Viability and caspase assays

A viability-, caspase 3/7- and caspase 9-assay were conducted, and the protocols for the assays were almost identical, thus they are described as one method. The assays are based on luminescence of analysis-specific molecules in the sample, and these molecules can bind or interact with the luminescent substrates in the reagent mixture. The viability assay measures the amount of ATP present, giving a measurement of metabolically active cells (Promega Corporation, 2012[c]). The substrates in the caspase assays are specific to caspase mediated cleavage, and they are luminogenically activated upon bond cleavage by caspases (Promega

3. Methods

Corporation, 2012[a] and 2012[b]). All cells used in these analyses were grown on transparent 96 well plates to differentiation and stressed by incubation with oxyrase for 0h, 2h, 4h, 6h or 22h.

Materials:

- CellTiter-Glo® Luminescent Cell Viability Assay

- Caspase-Glo® 3/7 Assay

- Caspase-Glo® 9 Assay

Method:

- The bottle with buffer was added to the bottle with substrate and incubated on the lab bench for at least 1h.

- Stress medium was removed from the plate and 100 µl DM was added to each well.

- The plate was allowed to equilibrate to room temperature for approx. 30 min.

- 100 µl reagent mixture were added to each well. The plate was gently mixed by swirling it on the lab bench.

- The entire volume from each well of the cell viability assay was transferred to a corresponding white walled 96 well plate after 10 min incubation at room temperature, while the caspase assays was allowed to equilibrate for 1h before transfer.

- The luminescence of each sample was measured in a plate-reading luminometer with a default Promega setting of the software for the given analysis.

- Statistical analyses for viability assay were carried out as paired Student's t-test between experimental variables, using all samples for the viability assay, two-tailed distribution and assumption of equal variance.

- For the caspase assays; A pooled standard deviation and average value of two experiments was calculated, and a paired 2 sample t-test was performed in Minitab using average, number of samples and pooled SD as inputs.

4. Results

4.1 Growth and differentiation of bovine skeletal muscle cells

4.1.1 The doubling rate of proliferating muscle cells

Muscle cells were counted and viability were analysed to investigate how fast the cells would grow, and to estimate how big proportion of the cells that would survive under normal growth conditions.
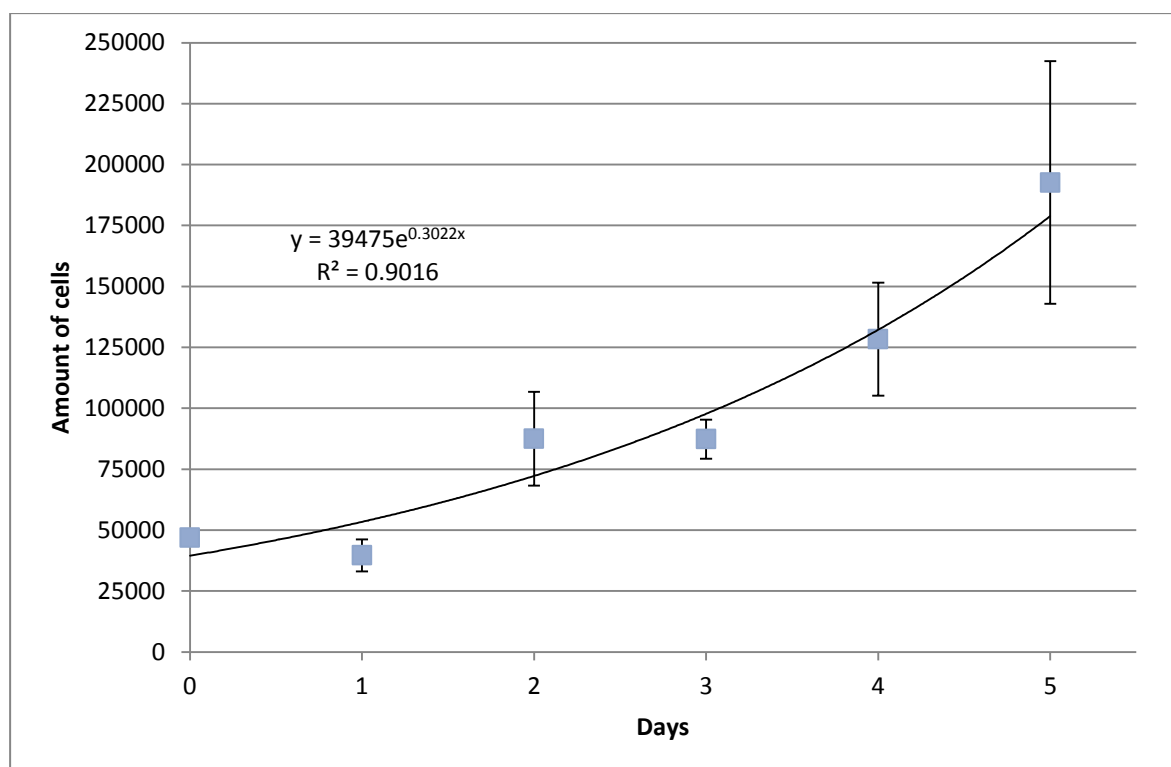

Figure 4.1: Cell proliferation over the time-course of 5 days. Average cell counting for 2 parallels, counted three times each, showing live cell count is presented. Error bars illustrates SD. The solid line is a logarithmic fit for living cells, with equation and R^2 values given in the upper left corner.

The muscle cells proliferate such that they are given relative good fit to an exponential model with R^2=0.90 (Figure 4.1). The equation corresponds to a doubling time for the cells of approximately 2.3 days. It can be seen that the cells need one day before they start growing sufficiently to increase in numbers. It can also be noted that standard deviations increase as cells increase in numbers.
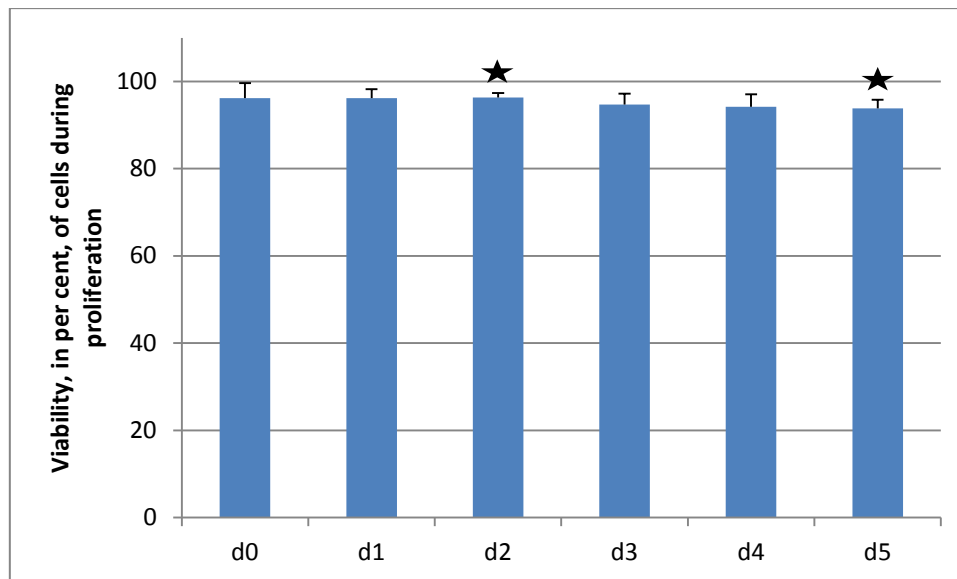
4. Results

Figure 4.2*: Viability in per cent of cells grown in PM over the time-course of 5 days. Values presented are the average cell viability for 2 parallels, counted three times for each parallel. There was significant difference between d2 and d5, indicated with asterisk, but no other significant differences. Standard deviation is illustrated by error bars.*

Viability of cells is essentially unchanged during a growth period of 5 days. There seems to be a trend towards a decrease in viability, since the average viability does decrease.

4.1.2 Myotubes are formed during differentiation

Muscle cells were photographed to give a visual representation of development during proliferation and differentiation.
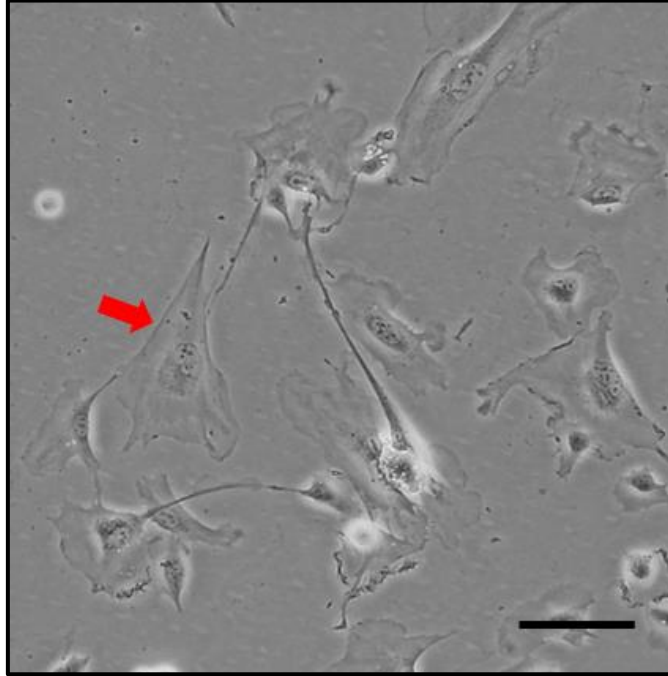

Figure 4.3: *Proliferating cells one day after seeding. Red arrow indicates the morphology of a proliferating myoblast. Scale bar equals 5 μm.*

Myoblasts was relatively dispersed during the first days when proliferating. Proliferating dispersed myoblasts has a characteristic triangular shape (Figure 4.3). Increased confluence of proliferating cells caused cell alignment and myoblasts adopt a more rectangular or elongated shape (Figure 4.4 A).
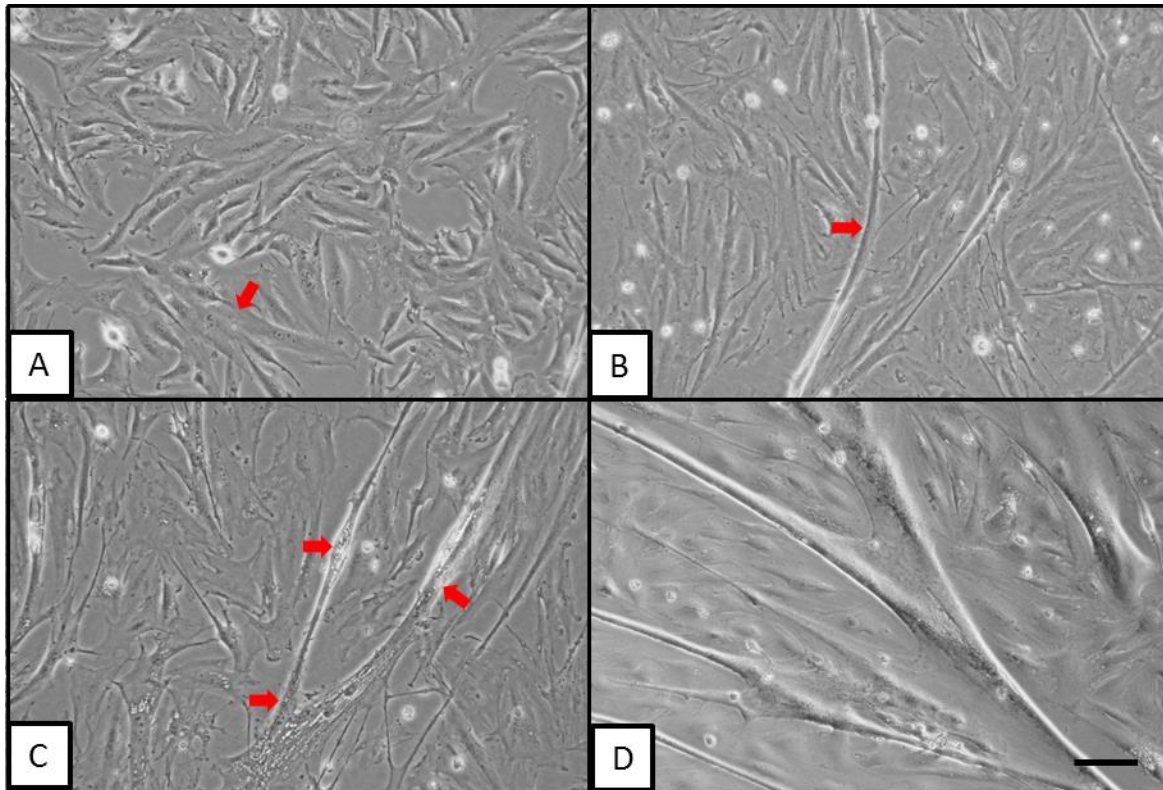
4. Results

Figure 4.4: *Development of muscle cells during proliferation and differentiation. The figure shows randomly chosen, representative images of cells after 2d (A) of proliferation, and cells induced to differentiation for 2d (B), 4d (C) and 6d (D).* ***A****: Arrow indicates aligning myoblasts.* ***B****: Arrow indicates a single myotube.* ***C****: Arrows indicates two connected myotubes. Pictures were taken at 10× magnification. Scale bar equals 5 μm.*

Cells cultivated for two days in PM showed little sign of differentiation (Figure 4.4 A), while those incubated in DM showed increased degree of differentiation with longer incubation times (Figure 4.4 B-D). The cells in DM for two days showed some degree of commitment to differentiation, but most of the cells seemed to be in the proliferating still (Figure 4.4 B). The amount of differentiated cells seemed to increase further at day four and the muscle cells had created networks of more than one filament (Figure 4.4 C). At day six the cells had created an interconnected set of filaments where it was hard to separate the individual filaments from one another (Figure 4.4 D). Even though many cells differentiated after 2-6 days, there were still many cells that remained proliferating, giving a heterogeneous cell distribution of proliferating and differentiated cells.

4.1.3 Localization of cytoskeletal proteins during differentiation

Investigation of cytoskeletal structure, by immunofluorescence microscopy of proliferating and differentiating cells, was done to give good understanding of these proteins under normal growth conditions.
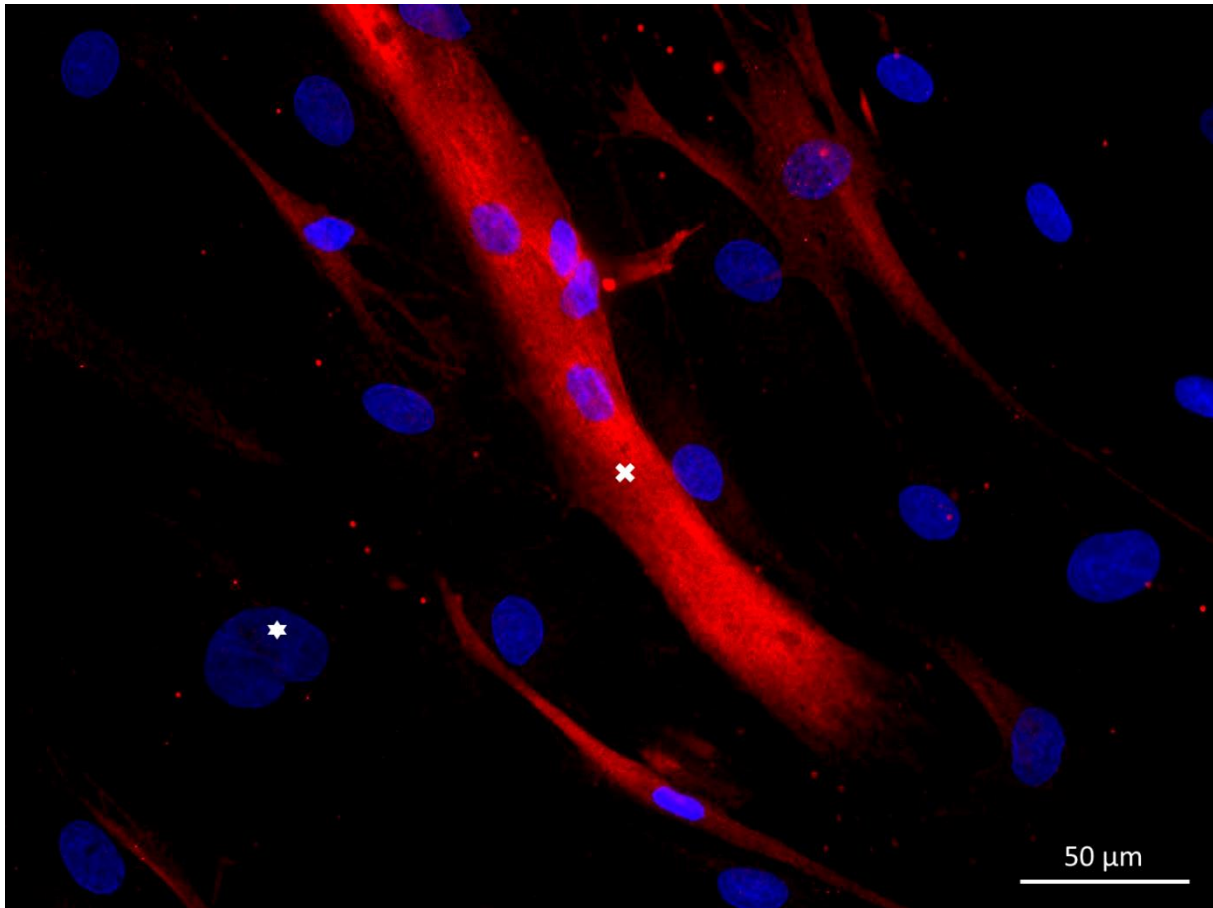

Figure 4.5: *Differentiating cells were fixed with 2 % PFA, immunostained with rabbit anti-Desmin, followed by DyLight 549-conjugated mouse anti-rabbit (red) before fluorescence microscopy analysis. White star shows a proliferating cell, where only the nucleus can be seen. The white cross shows differentiated cells, where more than one nucleus is clustered in addition to desmin filament formation. Nuclei were stained with DAPI (blue). Scale bar 50 μM.*

Myotubes were formed during differentiation (Figure 4.5). The myotubes contained more than one nucleus, and these were clustered together. Distinct desmin filaments were formed in myotubes. Proliferating cells show little or no desmin filament development and these cells contain only one nucleus.
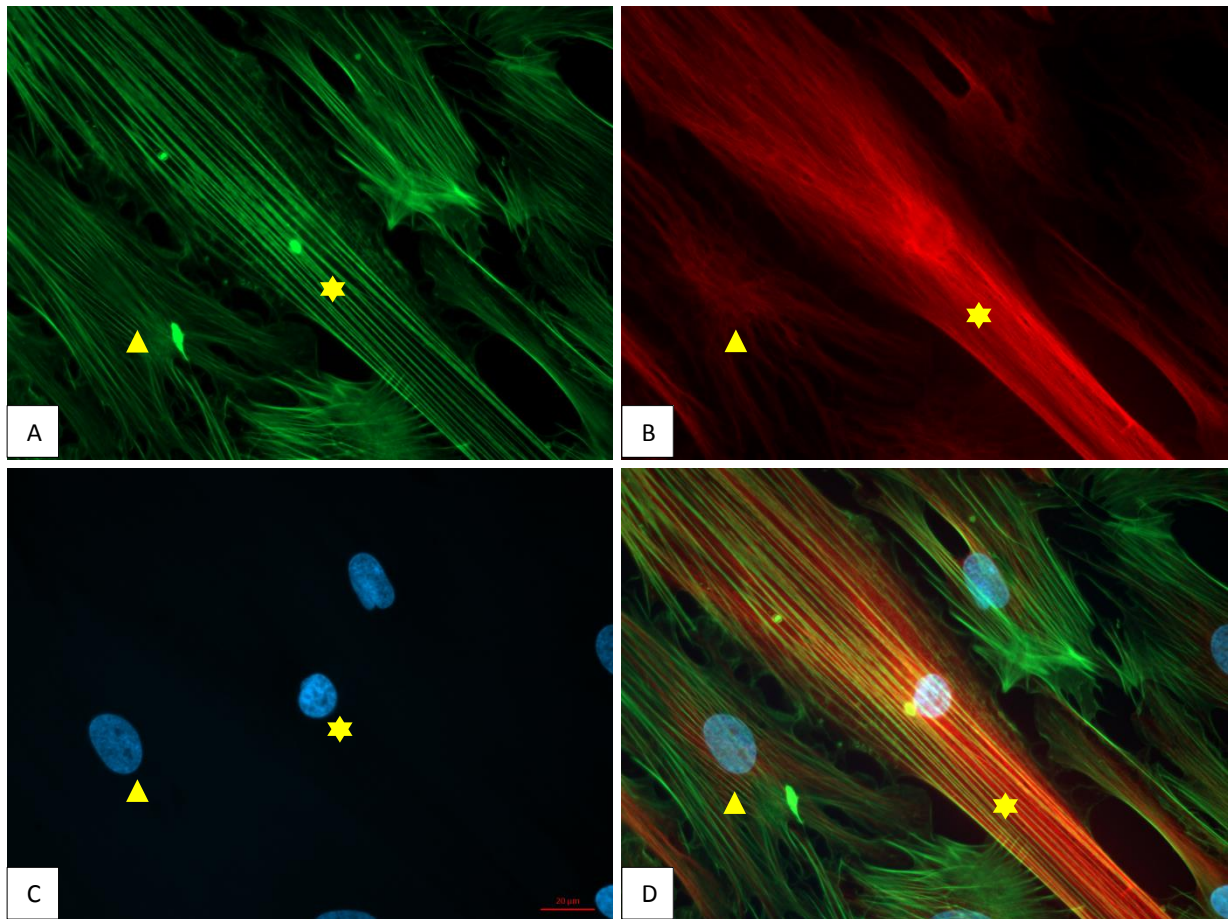
Figure 4.6: *Fluorescence microscopy analysis of cells immunostained with Alexa 488-Phalloidin (green), mouse anti-Tubulin, followed by Alexa 546-conjugated goat anti-mouse (red), and DAPI (blue) before fluorescence microscopy analysis. **A**: Actin. **B**: Tubulin. **C**: DAPI. **D**: merged. The cell marked with a yellow star has initiated differentiation. Cell marked with yellow triangle is still at the proliferating stage. Scale bar equalling 20 µm is shown in figure C.*

Actin and tubulin filaments seem to arrange in a linear and parallel manner, following the longitudinal direction of the myotubes, in differentiated cells (star in figure 4.6 A, B). These filaments in proliferative cells seem to have their origin in the centre of the cell, able to assemble in all directions (triangle in figure 4.6 A, B).

4.1.4 The mRNA expression of myogenic markers increased during differentiation

mRNA expression of four myogenic markers were investigated to give an impression of muscle cell development during incubation with DM.
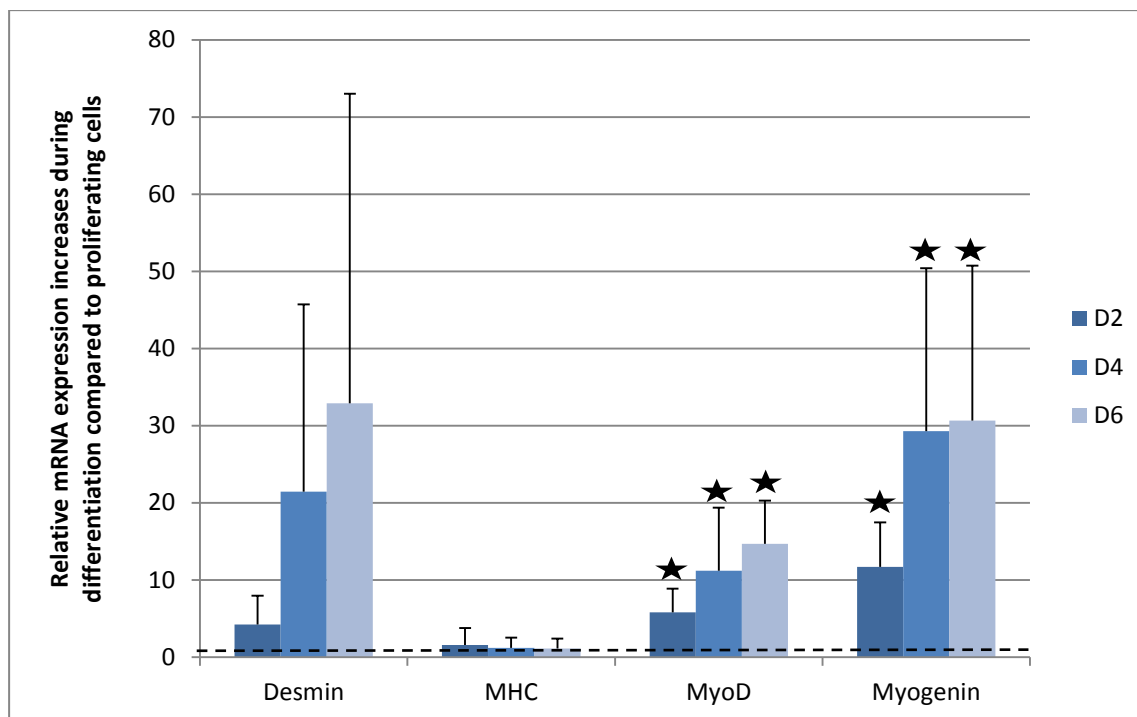
Figure 4.7: *Bars show the relative mRNA expression of myogenic markers in differentiating cells (D2, D4 and D6) compared to proliferating cells (which was set to 1, illustrated by the dashed line). The data are presented as the average of three independent experiments seeded out in two wells, and each real-time PCR performed in technical triplicates. Error bars illustrate SD. Asterisks denote significant differences between differentiation time and control for the given gene (*p<0.05,).*

The expression MyoD and myogenin increased during differentiation for 6 days (Figure 4.7), while MHC seemed to be unchanged during the period. The standard deviations were high for most mRNA transcripts, especially desmin, but the trend was an evident increase in relative expression of desmin during differentiation. Increase in MyoD and myogenin was significant compared to proliferating cells. We did not observe significant increase in mRNA expression for each myogenic marker between D2, D4 and D6.

4.1.5 The protein expression of myogenic markers increased during differentiation

Investigation of protein expression of myogenic markers allowed for validation that mRNA was translated to proteins.
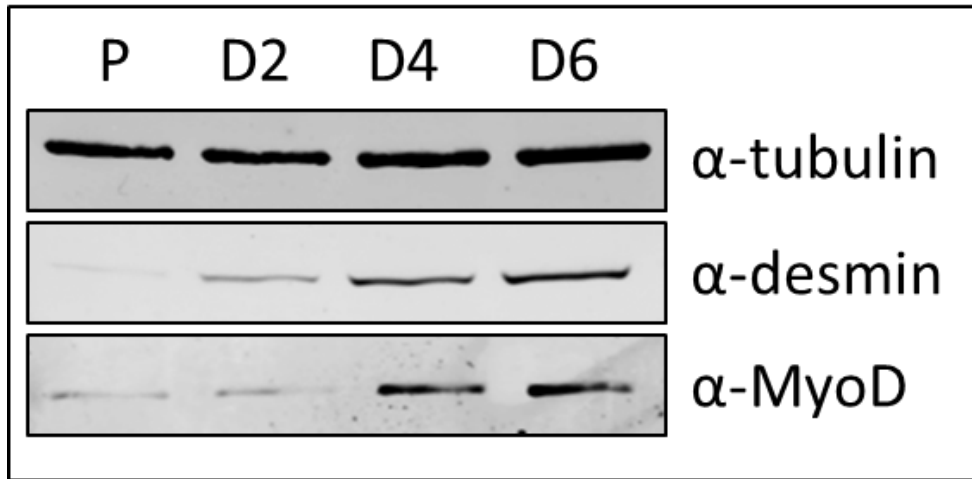

Figure 4.8: Representative western blot, showing cell lysates subjected to western blotting and stained with antibodies to tubulin (loading control), desmin and MyoD. P = 2d in PM and was used as control sample. D2, D4 or D6 = 2d, 4d or 6d in DM respectively after 2d in PM.

The protein expression of tubulin seems to be unchanged during differentiation, and is therefore suitable as a loading control. The protein expression of both desmin and MyoD seems to increase during the differentiation (Figure 4.8), consistent with the relative mRNA expression (Figure 4.7). The most dramatic increase in desmin and MyoD seems to be from D2 to D4 in these samples, with a further increase at 6D.
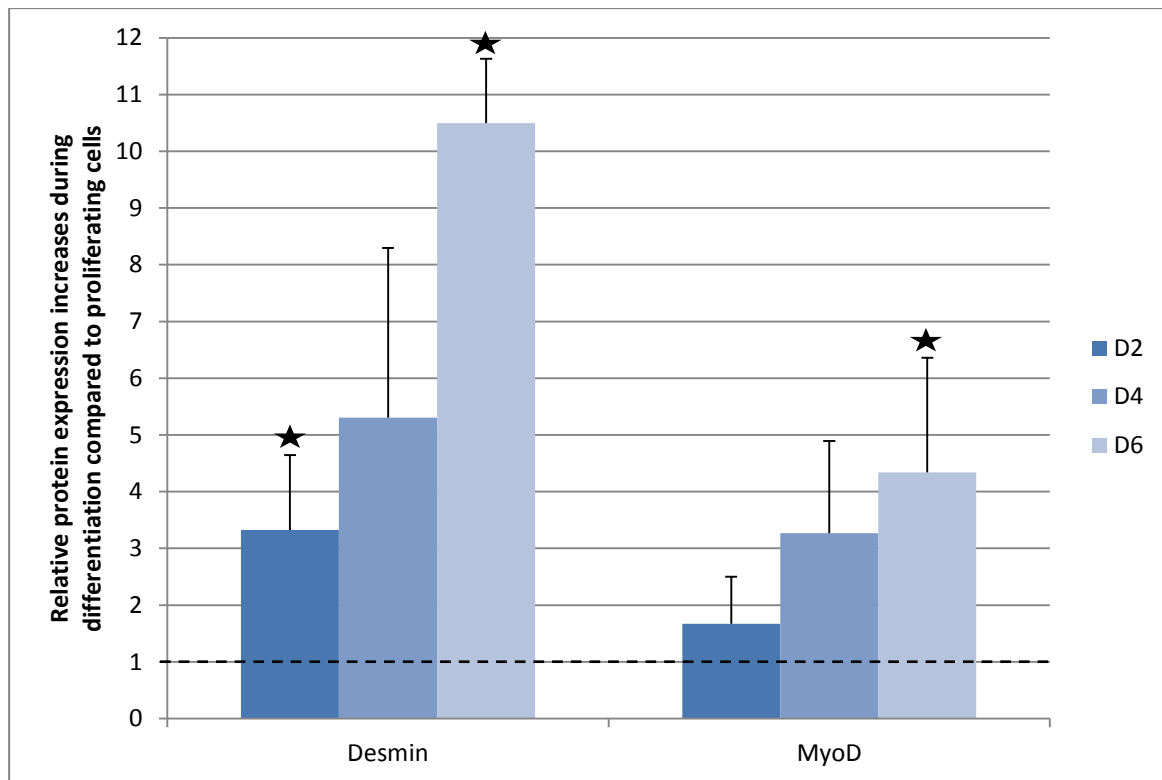
Figure 4.9: *Bars show the relative protein expression of myogenic markers in differentiating cells (D2, D4 and D6) compared to proliferating cells (which was set to 1, illustrated by the dashed line). Mean relative expression of desmin and MyoD are from 3 samples. D2, D4 or D6 = 2d, 4d or 6d in DM respectively after 2d in PM. Error bars illustrates SD. Asterisk denotes significant difference between given sample and the control for the given protein (*p < 0.05).*

Both desmin and MyoD protein expression increased during differentiation, and the expression was significantly increased for both proteins after 6 days of differentiation (Figure 4.9). Relative protein expression seemed to increase gradually from day to day.

4.2 Muscle cells showed signs of entering apoptosis when oxygen was removed

4.2.1 Oxygen removal induced detachment and degradation

Light microscopy was used to investigate if morphological changes would appear when oxygen was removed.
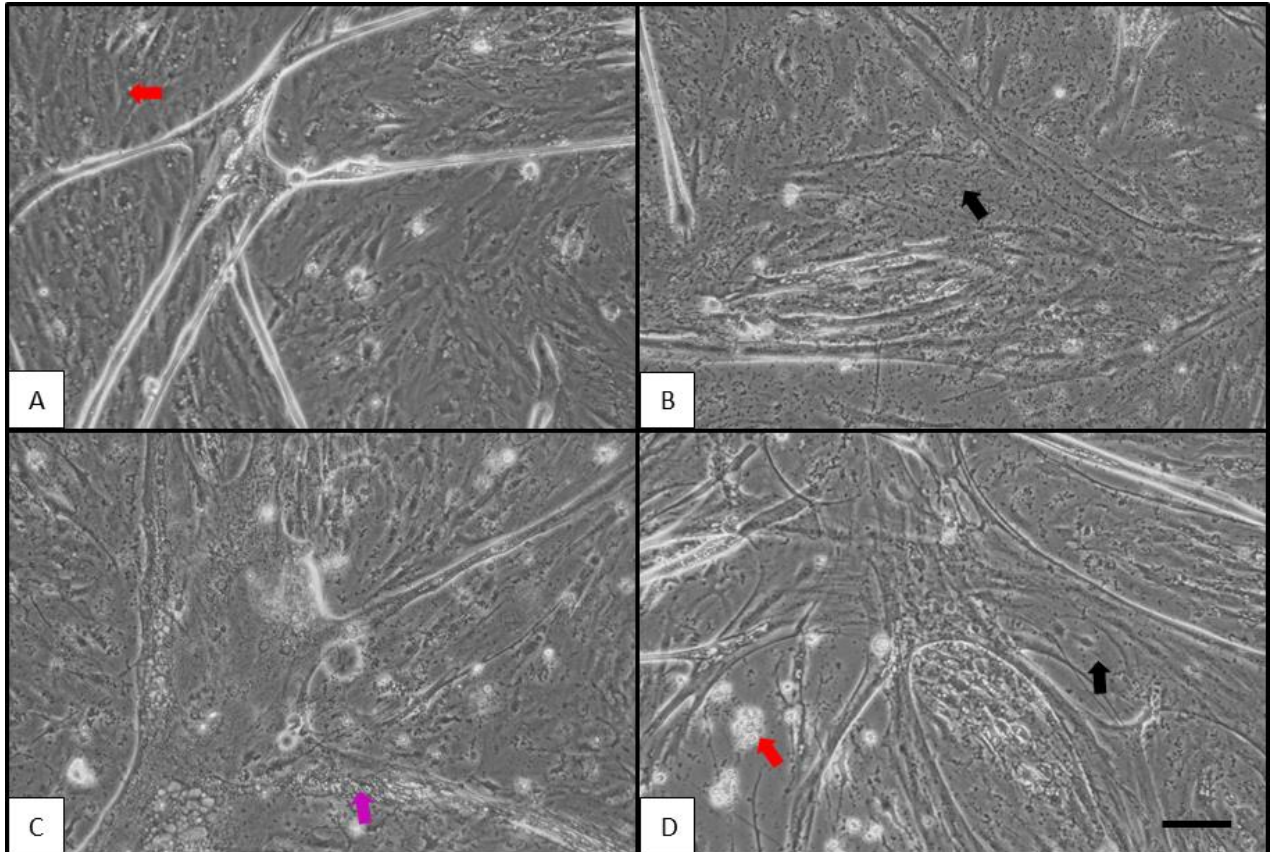

Figure 4.10: *Muscle cells incubated with oxygen removal for 0h (A), 2h (B), 4h(C), or 6h (D).* ***A****: Red arrow indicates aligned proliferating cells.* ***B****: Black arrow indicates degraded particles.* ***C****: Purple arrow indicates cytoplasmic membrane distortions.* ***D****: Red arrow indicates proliferating cells detached from the coating, while the black arrow indicates low concentration of degraded particles in vicinity of differentiated cells. Pictures were taken at 10× magnification. Scale bar equals 5 μm.*

Oxygen removal induced evident changes in the muscle cells, and it seemed that the proliferating cells exhibited the most dramatic modifications (Figure 4.10 A-D). This can be seen by the disappearance of proliferating cells in samples when oxygen was removed, while the differentiated cells seem to be more morphologically intact (Figure 4.10 D). The proliferating cells seemed to loosen from the ECL coating and float freely in the medium, seen as bright white circles after 6h (Figure 4.10 D). After 2h there can be seen many degraded particles in

intercellular spaces (Figure 4.10 B), these particles seemed to gradually disappear from the intercellular space within 6h after oxygen removal (Figure 4.10 C, D).

4.2.2 Mitochondrial membrane potential decreased following oxygen removal

JC-1 staining was used to investigate if the mitochondrial membrane potential would decrease following removal of oxygen.
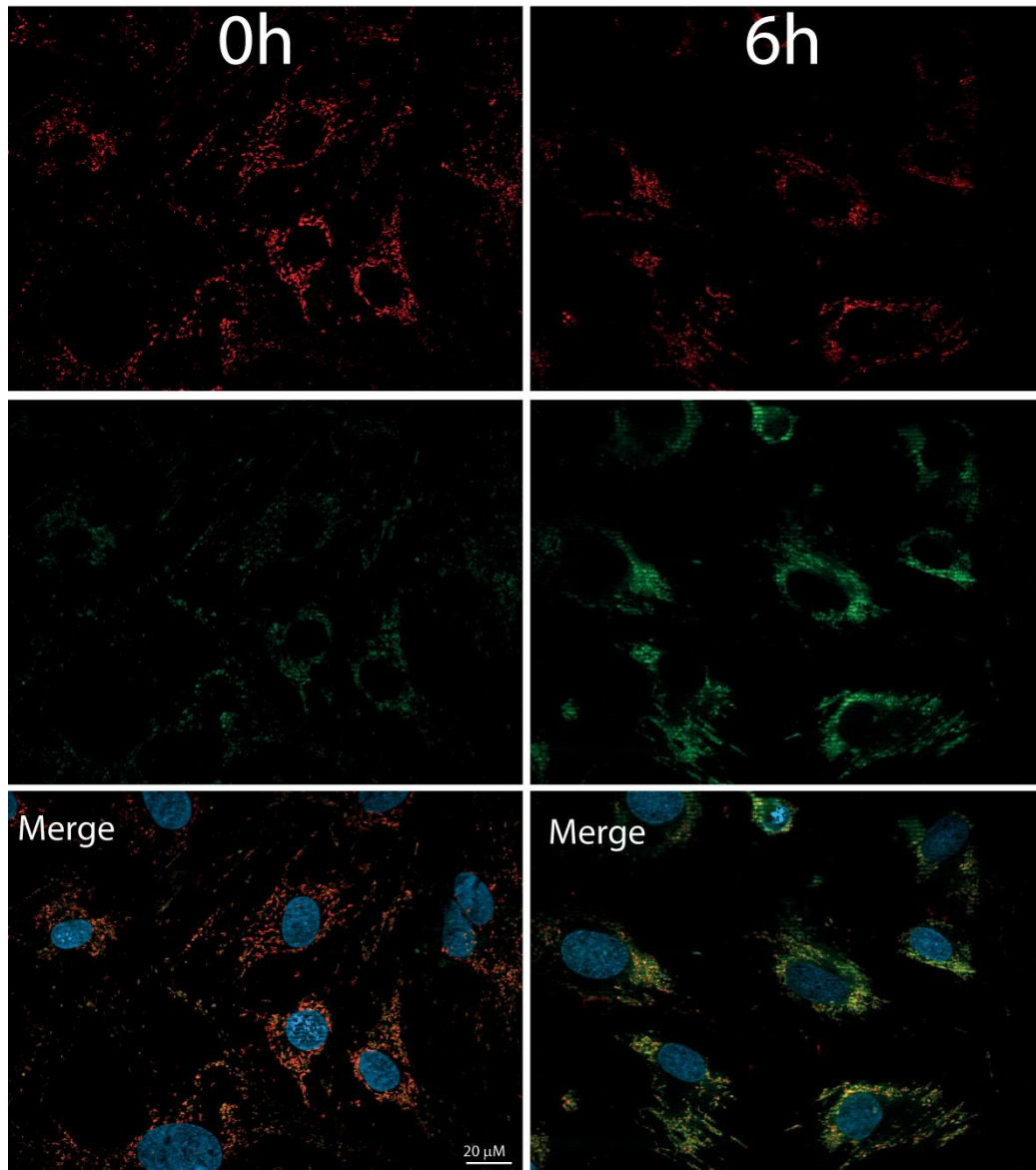

Figure 4.11: Live fluorescence microscopy analysis of cells treated with JC-1 dye before removal of oxygen. Red staining = normal function of mitochondria. Green staining = loss of mitochondrial membrane potential (indicator of apoptosis). All settings for microscope images were the same for both pictures.

4. Results

The ratio of green (apoptosis) to red (normal cells) seems to increase from 0h to 6h after removal of oxygen, by increasing the concentration of the green stain and simultaneously decreasing the concentration in red stain from 0h to 6h (Figure 4.11).
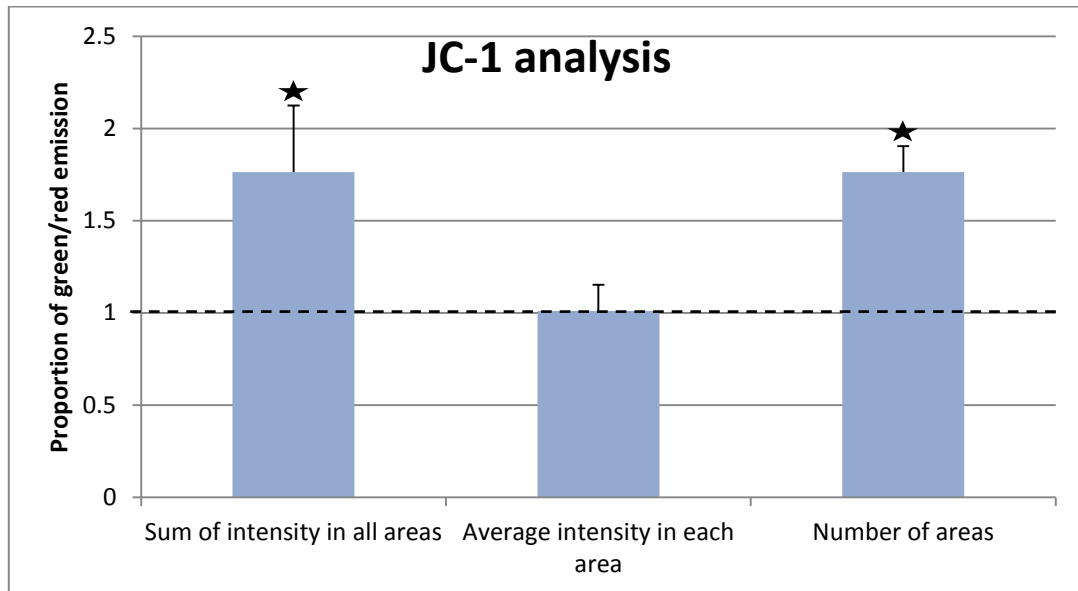
Figure 4.12: *Results from quantification of JC-1 from pictures taken at 0h and 6h, where 6h samples before removal of oxygen were used as control (which was set to 1, illustrated by the dashed line). Results are shown as the relative proportion of green emission versus red emission. 4 pictures were used for the control and 5 pictures for the sample incubated without oxygen for 6h. Error bars illustrates SD. Asterisk denotes significant difference between given analysis and the control (*p < 0.05).*

Quantification of pictures from JC-1 staining analysis shows that the relative total sum of emission and the number of green areas significantly increases from 0h to 6h (Figure 4.12). The average intensity in each detected area did not change from the 0h pictures to the ones taken at 6h.

4. Results

4.2.3 The relative mRNA expression of apoptotic markers increased

Early changes in apoptotic markers, within one hour of oxygen removal, were investigated first.

Figure 4.13: *Average relative mRNA expression of the genes Bax, Bcl2, Bim, Bid and Aif in cells incubated with medium where oxygen was removed for 15 min, 30 min, 45 min, or 60 min, compared to samples without removal of oxygen (which was set to 1, illustrated by the dashed line). Results are from two independent experiments, where real-time PCR were performed in technical triplicates. Error bars illustrates SD. Asterisk denotes significant difference between given sample and the control for the given gene (*p < 0.05).*

There were very minor changes in mRNA expression during the first hour after oxygen removal (Figure 4.13). Almost all samples were close to one in relative expression and there were few significant results, implying a small impact of experiment conditions. Following this analysis, longer times of incubation with removal of oxygen were investigated (Figure 4.14).
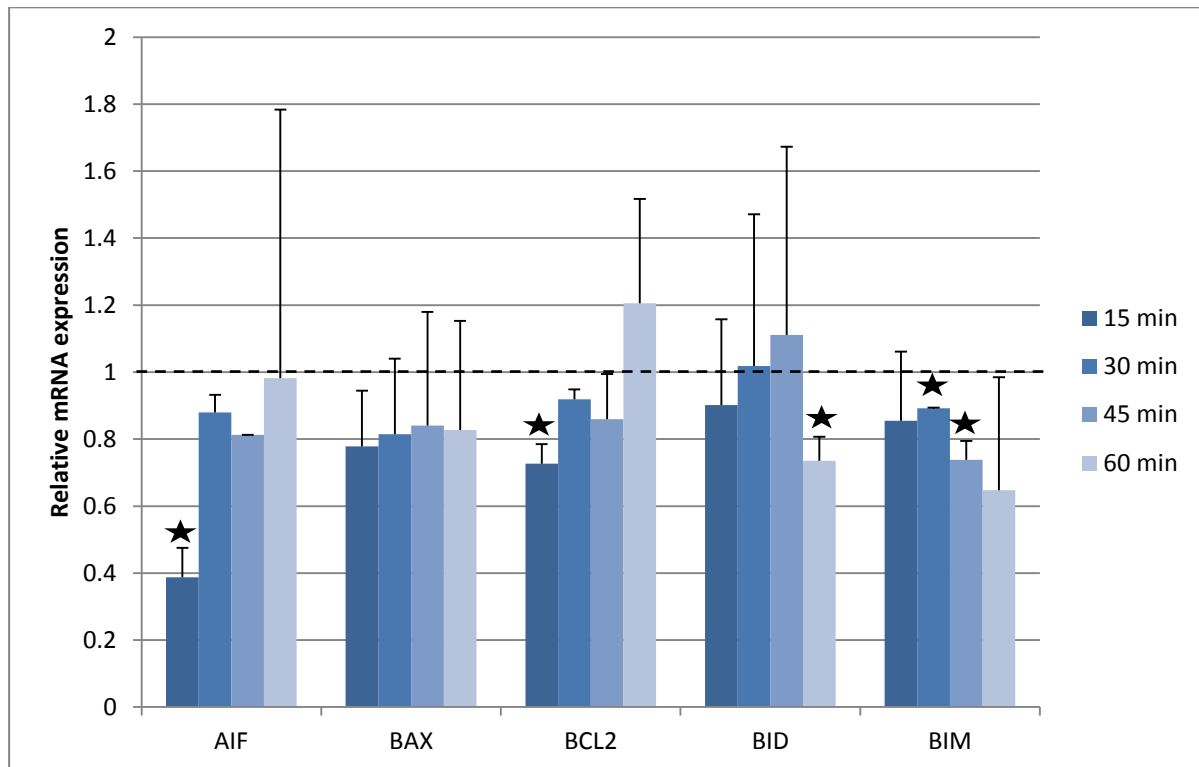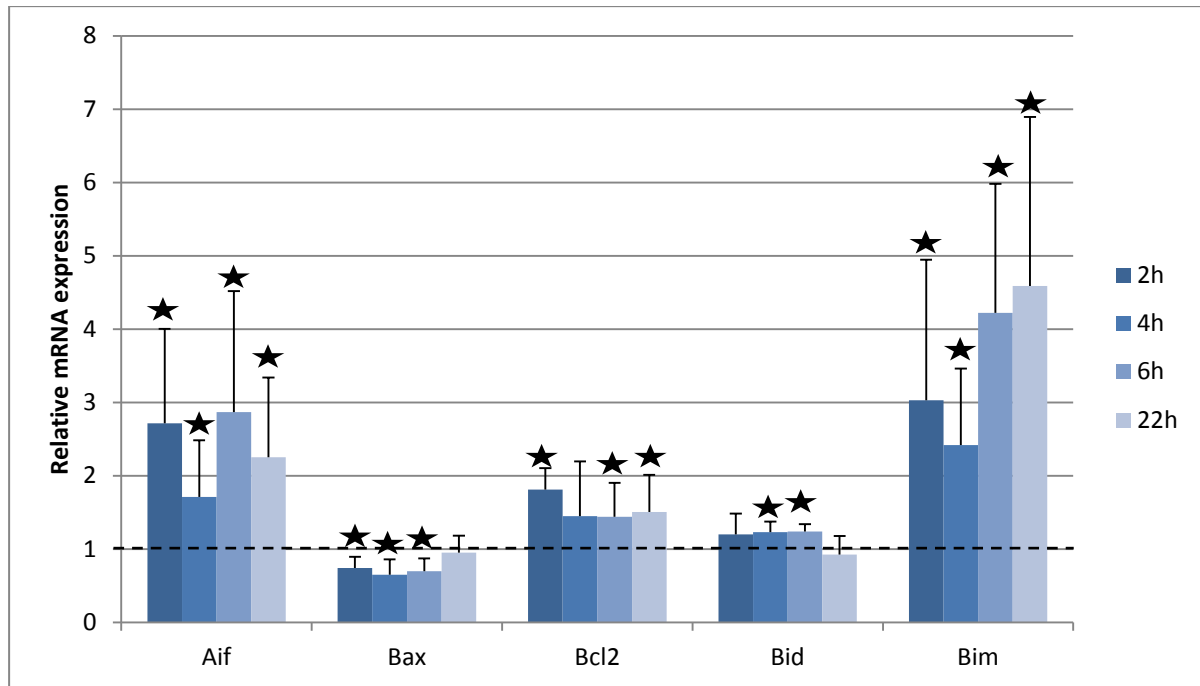
Figure 4.14: *Average relative expression of the genes Bax, Bcl2, Bim, Bid and Aif in cells incubated with medium where oxygen was removed for 2h, 4h, 6h, or 22h, compared to samples without oxygen removal (which was set to 1, illustrated by the dashed line). Results are from two independent experiments, seeded out in 3 wells each with real-time PCR performed in technical triplicates. Error bars illustrates SD. Asterisk denotes significant difference between given sample and the control for the given gene (*p < 0.05).*

Results show that all investigated gene expressions was impacted by removal of oxygen (Figure 4.14). Effects of oxygen removal were best seen in Aif and Bim, where all incubation times gave a significant increase in expression. Actin seemed to decrease, with a minimum expression at 6h. Bax was significantly decreased at all times investigated except at 22h. Bcl2 seemed to increase at all times investigated. There was a small, but significant, increase in Bid at 4h and 6h, while the 2h and 22h sample seemed to be unaffected.

4.2.4 The protein expression of Hsp70 and PARK7 was up-regulated

Protein expression of Hsp70 and PARK7 was investigated to see if the cells exhibited some of the known defensive mechanisms against cellular stress.

Figure 4.15: *Bands from western blotting with anti-tubulin, anti-PARK7 and anti-Hsp70. 0h = incubated without removal of oxygen. 2h, 4h or 6h samples were incubated in medium where oxygen was removed for 2h, 4h or 6h respectively.*

The blot (Figure 4.15) shows the same trends as the quantification (Figure 4.16), with a transient increase for both Hsp70 and PARK7. Tubulin seemed to be unaffected by removal of oxygen when analysed by western blotting.
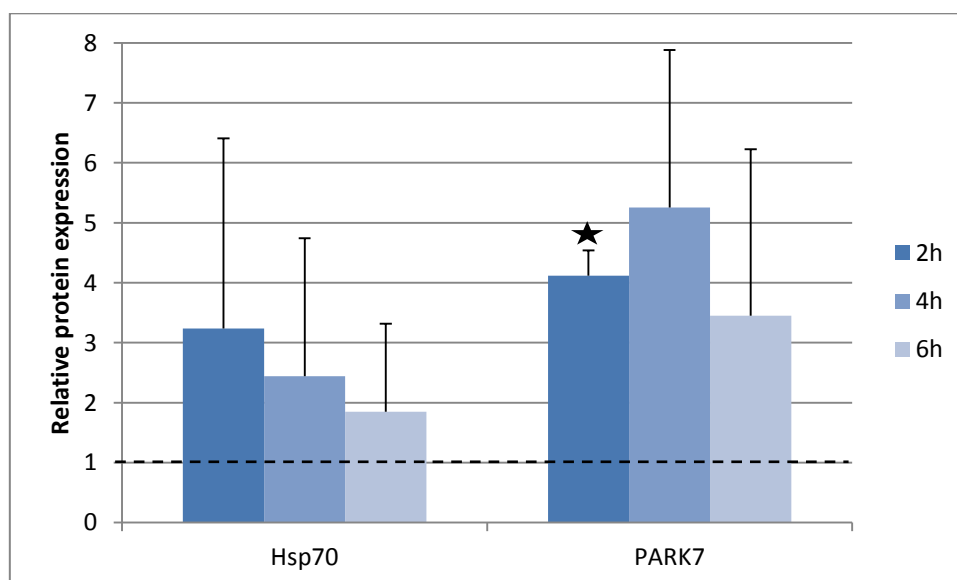
Figure 4.16: *Mean relative expression of Hsp70 and PARK7 for 3 biological parallels, with tubulin as control protein compared against the samples without oxygen removal (which was set to 1, illustrated by the dashed line). Error bars illustrates SD. Asterisk denotes significant difference between given sample and the control for the given protein (* p < 0.05).*

Both Hsp70 and PARK7 seemed to increase when incubated without oxygen, even though the only significant increase was for PARK7 after 2h (Figure 4.16). There seems to be a transient increase in PARK7 and Hsp70, where PARK7 has maximum concentration at 4h, while the concentration of Hsp70 was highest at 2h.

4.2.5. Oxygen removal induced cytoskeleton depolymerisation and degradation

Cytoskeletal changes were analysed by real-time PCR, immunofluorescence microscopy and western blotting to investigate the impact of oxygen removal.
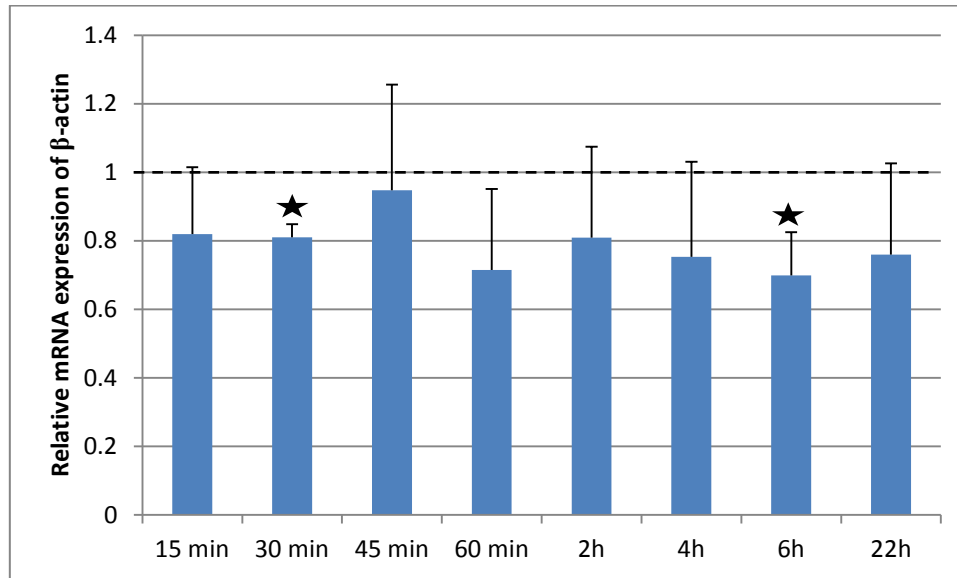
Figure 4.17: *Average relative mRNA expression of β-actin, incubated with medium where oxygen was removed for15 min., 30 min., 45 min., 60 min., 2h, 4h, 6h, or 22h, compared to samples without oxygen removal (which was set to 1). Results for samples designated 15 min, 30 min, 45 min and 60 min are from two independent experiments. Results for samples designated 2h, 4h, 6h and 22h are from two independent experiments, seeded out in three wells each. All real-time PCR were performed in technical triplicates. Error bars illustrates SD. Asterisk denotes significant difference between given sample and the control for the given gene (*p < 0.05).*

mRNA expression of actin decreased when oxygen was removed (figure 4.17). Expression reached the lowest at 6h, where it was significantly lower than the calibrator.
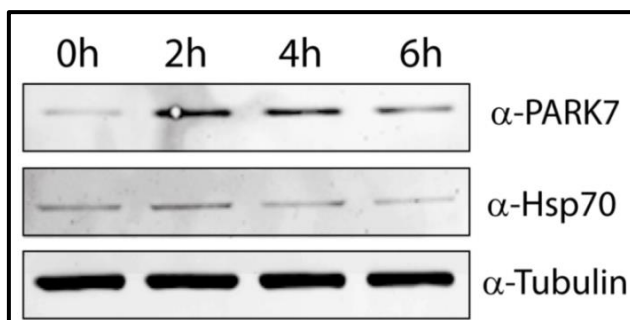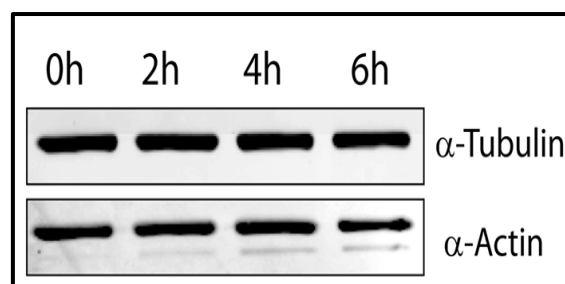

Figure 4.18: *Bands from western blotting with anti-tubulin and anti actin. 0h = incubated without removal of oxygen. 2h, 4h or 6h samples were incubated in medium where oxygen was removed for 2h, 4h or 6h respectively.*

Actin was cleaved when oxygen was removed, visualized by second band appearing gradually under the main band for actin (figure 4.18).
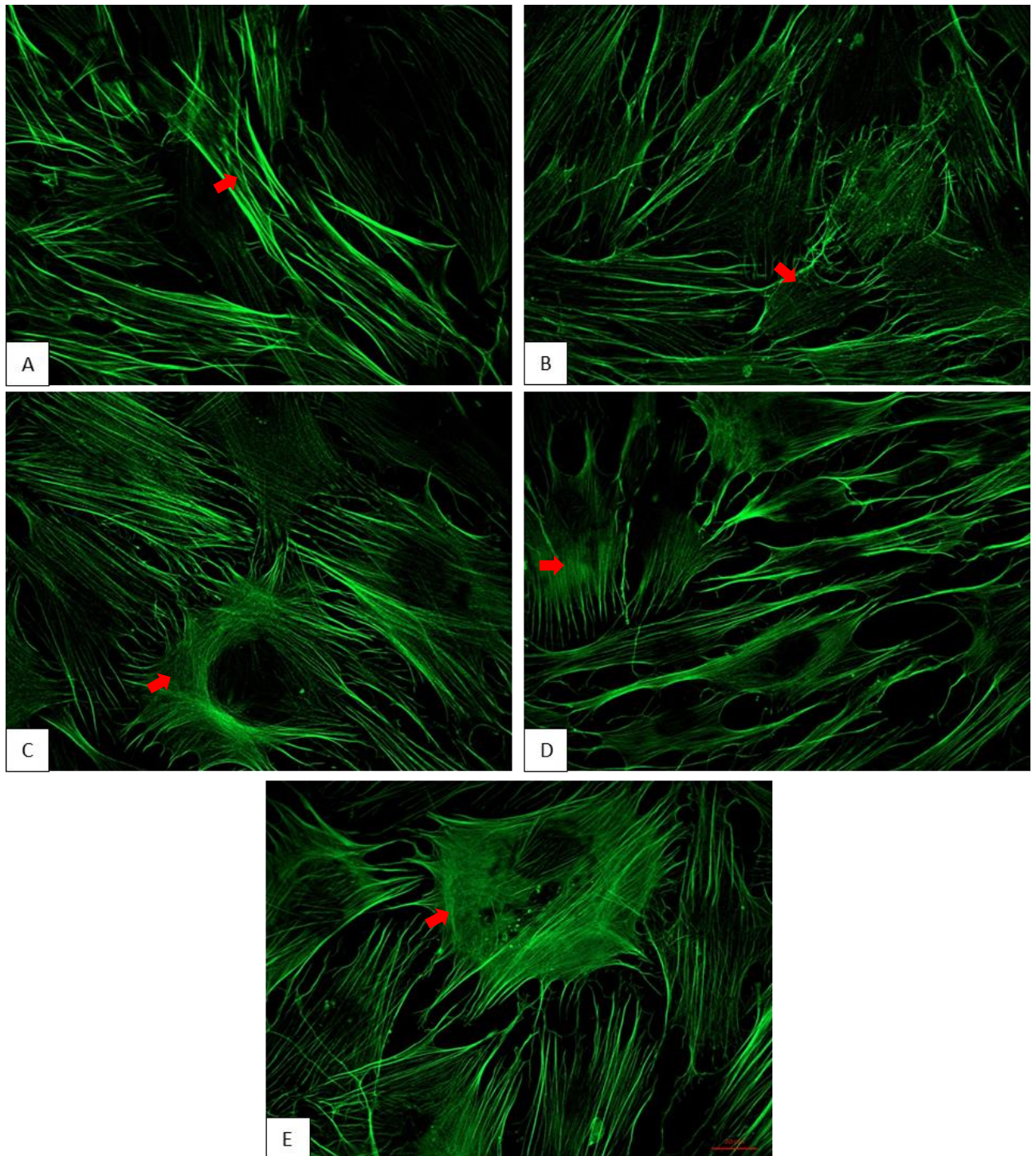
Figure 4.19: *Fluorescence microscopy analysis of differentiating muscle cells immunostained with Alexa 488-Phalloidin before fluorescence microscopy analysis. Cells were incubated with removal of oxygen for 0h (A), 2h (B), 4h (C), 6h(D) or 22h (E).* ***A****: Actin filaments were straight and coherent, indicated by an arrow.* ***B****: Actin filaments seemed to adopt a rougher shape,*

*indicated by an arrow. **C-E**: Actin filaments seemed to depolymerise, giving a more homogenous distribution of actin within the cells and forming a peripheral ring inside the cell, some of these cells are indicated by an arrow.*

Morphology of actin polymers was normal in samples with available oxygen (Figure 4.19 A), showing distinct and uniformly distributed filaments. After removal of oxygen the actin filaments seemed to become less distinct, and many filaments seemed to redistribute within the cells (Figure 4.19 B-E).
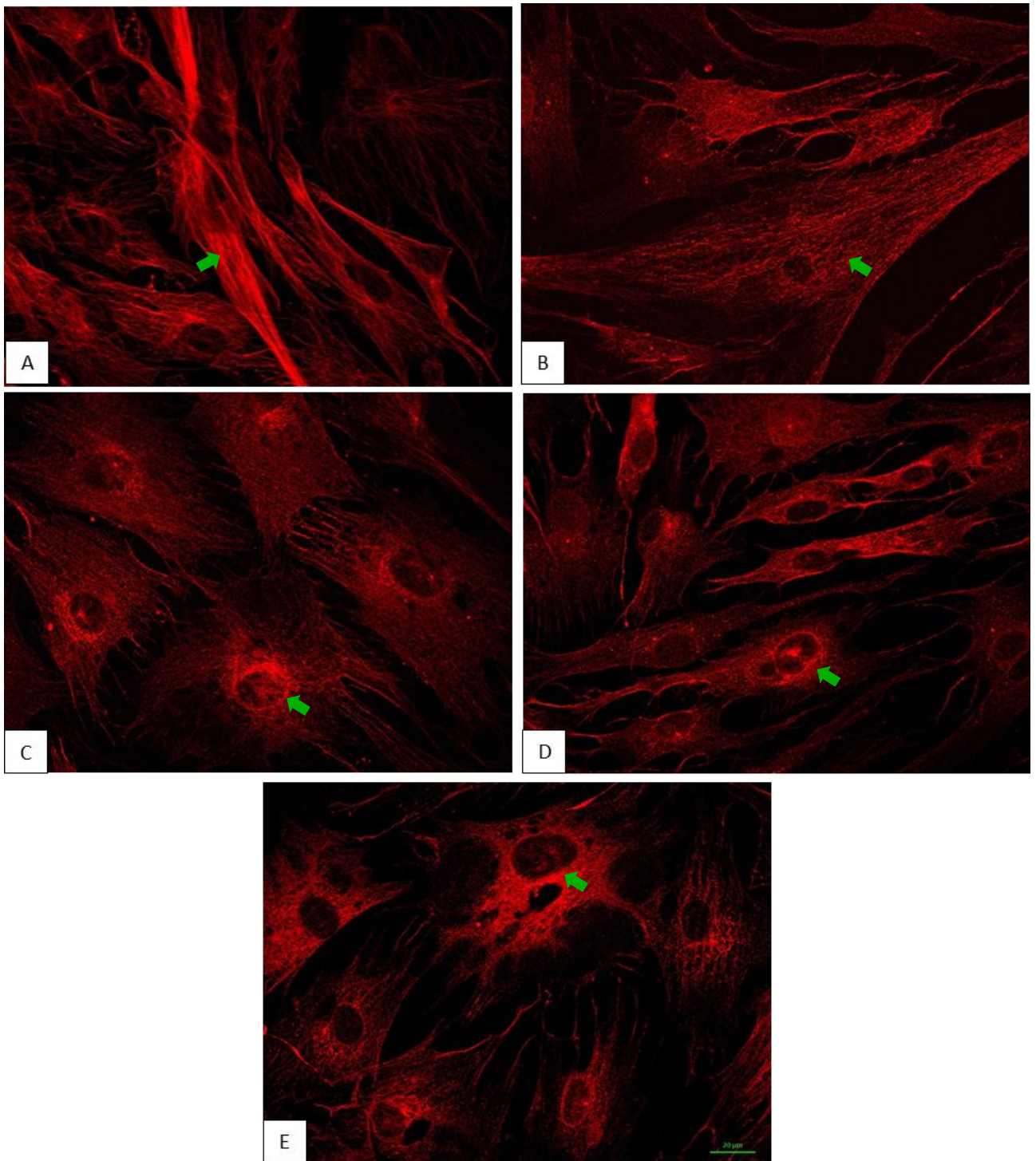
Figure 4.20: *Fluorescence microscopy analysis of differentiating muscle cells immunostained with mouse anti-Tubulin and Alexa 546-conjugated goat anti-mouse before fluorescence microscopy analysis. Cells were incubated with removal of oxygen for 0h (A), 2h (B), 4h (C), 6h(D) or 22h (E).* ***A:*** *All cells seemed to have normal tubulin filaments; a differentiated cell is indicated by an arrow.* ***B:*** *Depolymerisation of tubulin is evident, but distribution of tubulin within the cell seemed to be even, as in the cell indicated by an arrow.* ***C-D:*** *Tubulin seemed to be further depolymerised and localize near the cell nucleus, as in cells indicated by an arrow.* ***E:***

Depolymerised tubulin seemed to up-concentrate in parts of the cells, giving areas without tubulin and possible membrane blebbing, as in the cell indicated by an arrow.

Morphology of tubulin polymers was normal in samples with available oxygen (Figure 4.20 A). Tubulin polymers showed distinct signs of depolymerisation as early as after 2h (Figure 4.20 B). The depolymerisation seemed to commence further as time without oxygen elapsed, and depolymerised tubulin seemed to congregate near the nucleus (Figure 4.20 C-E). Blebs with high concentration of tubulin were observed after 22h (Figure 4.20 E).

4.2.6 Viability of cells decreased after prolonged removal of oxygen

Viability analysis was used to investigate if cells died when oxygen was removed from the incubation medium.
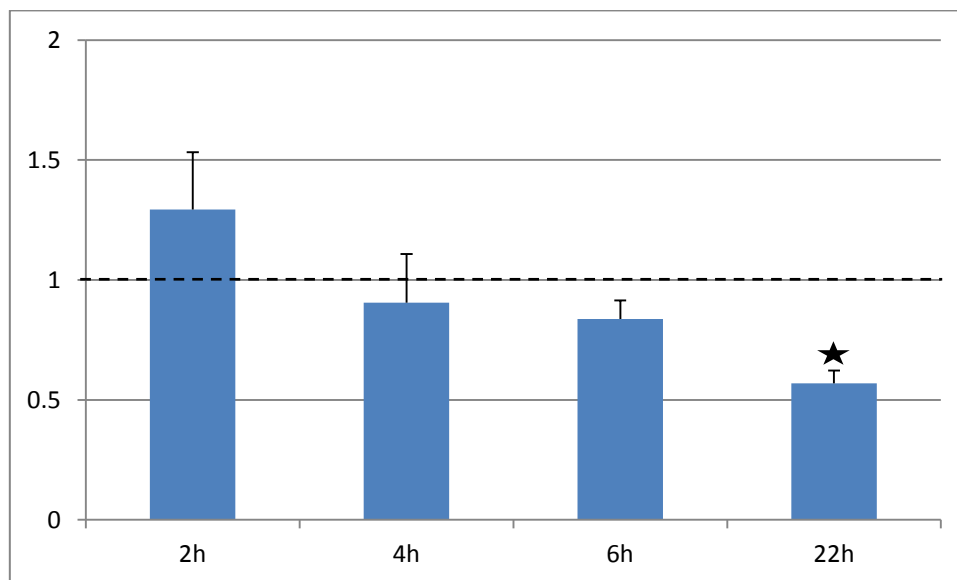
Figure 4.21: Results from viability assay, where luminescence is compared to the sample without oxygen removal (which was set to 1, illustrated by the dashed line). Results are from one experiment, seeded out in 5 wells for each incubation time. Error bars illustrates SD. Asterisk denotes significant difference between given sample and the control (*p < 0.05).

There appeared to be a decline in cell viability from 2h to 22h, but the only significant decrease was at 22h (Figure 4.21). It is worth noting that viability seemed to increase at 2h with oxygen removal.

4.2.7 Caspase concentration decreased after removal of oxygen

Caspase assays gave an opportunity to investigate if caspases were up-concentrated in response to oxygen removal.
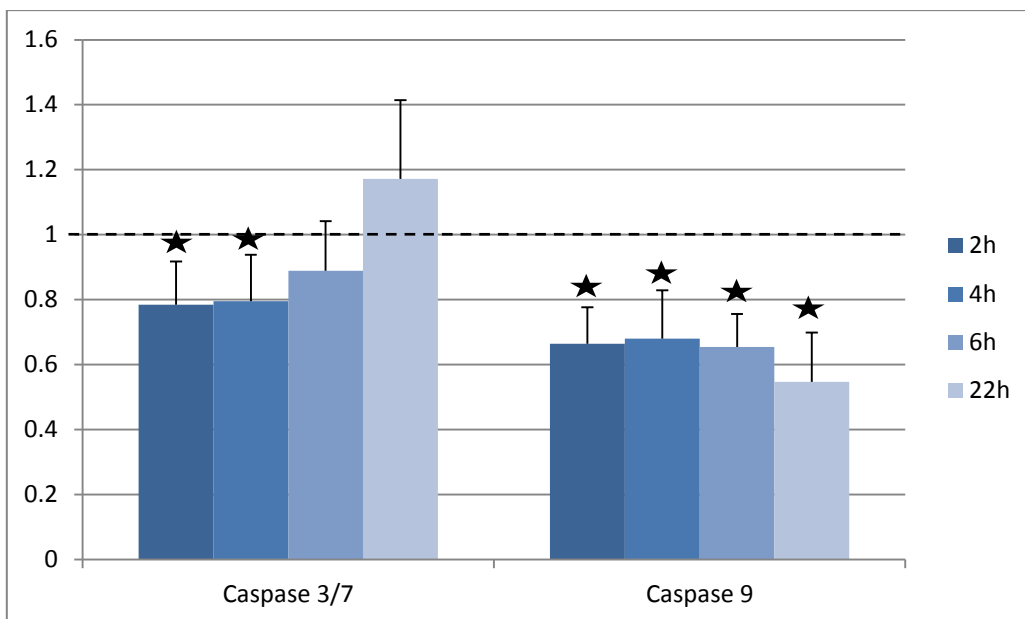
Figure 4.22: *Results from caspase 3/7 and caspase 9 assays, where luminescence was compared to the sample without oxygen removal (which was set to 1, illustrated by the dashed line). Results are from two experiments, seeded out in respectively 5 and at least nine wells for each incubation time. Error bars illustrates pooled SD. Asterisk denotes significant difference between given sample and the control (*p < 0.05).*

Caspase 9 concentrations were significantly reduced by removal of oxygen at all times investigated. Capase 3/7 decreased significantly at 2h and 4h (Figure 4.22). The concentration seemed to increase at 6h and further at 22h, to a value above the control, but these results were not significant when compared to the control sample.

5. Discussion

5.1 Growth and differentiation of bovine skeletal muscle cells

This first part was conducted to give an introduction to methods later used in the stress experiments, and was as such in line with established theory of satellite muscle cell behaviour.

5.1.1 Doubling rate and viability of proliferating muscle cells

From cell counting's and viability measurements it could be confirmed that the growth conditions for isolated muscle cells were good, because of an observed logarithmic growth and few significant changes in viability. Meaning that current basic PM, incubation temperature, CO_2 concentration in incubation chamber and seeding procedures were sufficient for further experiments. The decrease in cell numbers from day 0 to day 1 suggests that not all of the cells attach to the surface and that the cells need about a day to start proliferating. The cells were only followed for five days and further development beyond this time-period, under similar conditions, are uncertain. The cells will certainly not be able to divide infinitely, due to space and nutrition limitations, and will likely stop at a threshold, where both growth and viability probably will decline. Given that cells from these experiments double in numbers approximately each 2.3 days, the cells in this experiment had divided an average of two times. This is certainly within the Hayflick limit of doubling for animal cells, which is approximately 50 doublings of a fibroblast cells *in vitro* (Hayflick, 1979), and it is therefore likely that the muscle cells used in these experiments are still viable, with the assumption that the cells have not divided too many times in the live animal prior to isolation. Another consideration regarding cell passages is that the isolated satellite cells will contain some number of fibroblasts, and these cells will outnumber the muscle cells after numerous passages (Rønning et al., 2013).

5.1.2 Cell morphology during development

Cells cultivated in these experiments displayed good ability to both proliferate and differentiate under given conditions, which furthers the assumption that the protocols used are applicable for later experiments. These morphological analyses gave a good understanding of myogenic development of *in vitro* cultivated bovine satellite muscle cells, needed to determine when to induce cells for differentiation and when to stress cells in later experiments. This was important to investigate because satellite cells are known develop differently, e.g. how fast myosin is formed and their ability to differentiate, on the background of factors such as: age of animal from which satellite cells are isolated (Carlson et al., 2008), how the different growth mediums are

composed (Danoviz and Yablonka-Reuveni, 2012), and which muscles the culture is prepared from (Barjot et al., 1995).

5.1.3 Cytoskeletal and contractile proteins during differentiation

The proliferating cells had virtually no desmin, shown by immunofluorescence microscopy analysis, which is expected since these cells have not formed myotubes and has no other direct connection with other cells, giving no need for desmin filaments in early muscle development as detailed by Paulin and Li (2004). Upon differentiation and myotube formation, desmin filaments were likely assembled to connect and reinforce the structure of cells within the myotube (Carlsson and Thornell, 2001). Quantitative real-time PCR and western blot analyses strengthened the impressions from immunofluorescence analysis, i.e. an increase in desmin as cells differentiate. Even though the only significant increase was seen in western blot analysis, the real-time PCR showed an evident increase. The lack of significant results in real-time PCR can stem from the fact that it is a sensitive method and it is very difficult to harvest cells with the exact same proportion of proliferating and differentiating cells, and the cells can develop in different rates between experiments, giving variation between each seeding not easily controlled when sampling at given days.

Actin and tubulin expression seemed unchanged during proliferation and differentiation, but their filament organization changed during myotube formation. The observed parallel arrangement of actin filaments in differentiating cells is likely an adaption to be able to contract at later cell stages (Ono, 2010). Tassin et al. (1985) documented that microtubule organization changed from an unorganized fan-like distribution, with a centre at the nucleus, in proliferating cells to a parallel organization in myotubes, and this phenomenon was confirmed in the present study. MHC mRNA expression did not change during six days of differentiation, which is likely since these proteins are detected at later stages of differentiation. Barjot et al. (1995) showed that rabbit muscle satellite cells, cultured *in vitro,* expressed MHC first after 13 days of differentiation.

5.1.4 Myogenic regulatory factors

 Since both MyoD and myogenin increased significantly during differentiation, it can be hypothesized that they both are important for this process. Myogenin is known to be important during differentiation (Meadows et al., 2008). We were unable to detect Myogenin protein expression on western blot although an antibody that had previously worked well on immunofluorescence was used (Rønning et al., 2013). MyoD, on the other hand, is a somite

myogenic commitment factor (Rudnicki et al., 1993), in addition to impacting activation of satellite cells, proliferating cells and differentiation (Yablonka-Reuveni and Day, 2011). Jin et al. (2007) postulated that MyoD might work as a molecular switch, turning on differentiation. Other studies have also confirmed an important role of MyoD during cell cycle arrest (Cenciarelli et al., 1999) or by up-regulating myogenin to initiate differentiation (Yablonka-Reuveni et al., 1999). These findings, taken together with the discovery that MyoD seems to be most important during the first round of DNA replication after activation of satellite cells during proliferation (Zhang et al., 2010), gives reason to believe that MyoD expression will increase at early stages of differentiation when comparing against proliferating cells. Another element that could impact MyoD in samples is that the samples induced to differentiate still contained many cells that was still proliferating, possibly giving a higher total MyoD expression.

5.1.5 Summing up

Isolated satellite muscle cells were able to proliferate and differentiate under experimental conditions, as shown by cell counting during proliferation, expression of myogenic regulatory factors, microtube formation and reorganization of cytoskeletal proteins.

5.2 Oxygen removal caused cells to adopt an apoptotic phenotype

One of the first objectives is to determine whether oxygen was completely removed from the incubation medium. We did not measure concentrations of dissolved oxygen in the medium during stress experiments, thus the indirect signs of oxygen removal needed to be assessed. Yun et al. (2005) found that myogenesis in C2C12 cells was only mildly affected by oxygen levels as low as 0.5 % for three days, but that the impact was more severe at 0.01 % O_2, and that the muscle cells were still viable at this low oxygen concentration. This leads to the assumption that our system had oxygen concentrations in a range of 0.01 % or below, due to the decreased cell viability and overall damage exerted upon the cells.

Early changes in muscle cell morphology after removal of oxygen were appearance of degraded cell components, which may be large apoptotic bodies containing membrane enclosed cellular residues. The myotubes seemed to be less affected than the proliferating cells when analysed with light microscopy. This can be attributed to an increase in relative concentration of X-linked inhibitor of apoptosis protein (XIAP) to Apaf-1 in myotubes, thus XIAP can effectively inhibit Apaf-1 activation in myotubes (Smith et al., 2009). Since cells seemed to loosen from the coating at later stages of incubation, there was not expected considerable evidence of late stage apoptosis, e.g. stages of cellular condensation or fragmentation.

5.2.1 Mitochondria are important for initiating apoptosis in bovine satellite muscle cells

Decrease in mitochondrial membrane potential at six hours after oxygen removal, analysed by JC-1 staining, indicates induction of apoptosis (Green, 2011). The observed relative increase was caused by a shift from red to green emission in the detected areas, as the total number of green areas increased with a corresponding decrease in red areas from 0h to 6h after oxygen removal. The average intensity in each area was unchanged, and the total sum of green/red intensity did likewise increase, as expected by the two other findings.

The finding that mitochondrial membrane permeability increases at 6h after oxygen removal is supported by the observed relative changes in mRNA expression of Bcl2-family of proteins at, where the pro-apoptotic transcripts increase more than the anti-apoptotic at 6h. Assuming these interact in an approximate one-to-one fashion (Vaux, 2004), the pro-apoptotic protein Bim could alone be responsible for an effective silencing of anti-apoptotic Bcl2, by increasing two times as much as Bcl2, resulting in reduced apoptotic protection of the mitochondrion. Bax and Bid, the

two other pro-apoptotic genes, was relatively unchanged, leading to an assumption that Bim is the primary pro-apoptotic gene of the three investigated in this system.

The increase in mRNA expression of Aif can also support this finding, even though the directly transcribed/translated Aif protein is not apoptogenic (Susin et al., 1999). This means that increase in mRNA expression of Aif is not necessarily linked to mitochondrial release of Aif or effective translocation to the nucleus. On the other hand, it can be hypothesized that increase in AIF mRNA is a response to the release of mitochondrial Aif, done to replenish the lost Aif in mitochondrion.

Intrinsic factors mediated by mitochondrial membrane alterations and release of pro-apoptotic proteins seemed to be most important in this cell system, which is likely due to the fact that extracellular ligands and granules will be at a minimum in an *in vitro* cell system.

5.2.2 Cytoskeletal re-organisation impacts the timing of apoptotic events

Breakdown of tubulin and actin filaments during apoptosis can come from different sources, such as lack of energy or breakdown by caspases.

Microtubules are known to disassemble early in during the effector phase in apoptosis, but the mechanism is unknown (Mills et al., 1999), and this was observed at all investigated times of oxygen removal. Moss et al. (2006) showed that microtubules are re-formed during later stages of apoptosis to facilitate cell fragmentation, which was observed in this study at 22h after oxygen removal. Total tubulin seemed to stay the same during experiments when analysed by western blotting, suggesting no breakdown of tubulin monomers, suggesting that main influence of oxygen removal is by affecting filament reorganization.

Actin is a known substrate for caspases and a key indicator of apoptosis (Kemp and Parr, 2012), and it's known to re-arrange in the early stages of apoptosis (Mills et al., 1999). Both breakdown and re-arrangement of actin were observed in this study, analysed by western blot and immunofluorescence microscopy respectively. Reduction in mRNA expression of actin suggests that the cells emphasise their energy expenditure at other processes than cellular construction and proliferation, or the reduction could be caused by direct effect of Aif on the DNA, by digesting actin specific DNA. Actin and myosin are important for bleb formation during apoptosis (Mills et al., 1999), and the lack of myosin, specifically MHC, in our cell system could be the reason for few detected blebs on cells.

The process of apoptosis is not strictly coordinated between cells (Herrera-Mendez et al., 2006), which means that all stages of apoptosis could be present at the longer incubation times without oxygen and that the amount of cells affected could vary independent of incubation times. This can explain some of the larger variations between samples.

5.2.3 Protective proteins delay caspase activation

The decrease in effector caspases 3 and 7 during the first few hours of oxygen removal in these experiments can in part be contributed to the increase in protective proteins, such as Hsps and PARK7 (see section 1.2.5 for details). Supporting the increase in Hsps is a study by Yang et al. (2012), who also found an up-regulation of Hsps in muscle cells where hypoxia was chemically induced. Once these protective proteins decrease in concentration, the caspases can be activated and cell suicide can commence, and the protective proteins seem to correlate in an inverse manner with caspase 3 and 7 concentrations in the present study.

The relative high concentration of caspase 3/7 and 9, as seen when comparing cells without removal of oxygen to cells where oxygen was removed, can be attributed to the fact that these caspases are involved in the differentiation process (Fernando et al., 2002, Murray et al., 2008), and the caspases may therefore be active before oxygen was removed. The decrease in caspase 9 activity, after oxygen removal, can be seen as contradictory to an effective induction of apoptosis, since this caspase is needed to activate caspase 3 and 7 (see section 1.2.1.3 for details). One possible explanation for this can be that caspase 9 concentration was elevated at times not investigated, e.g. between 6h and 22h after removal of oxygen, to plummet after successful activation of the effector caspases.

Another explanation for decrease in caspase concentrations, as seen in caspase 9, can be the fact that cell viability decreases following removal of oxygen, meaning that some of the cells die and loosen from the ECL coated surface. This means that the dead cells will be removed from the well before addition of caspase assay reagents, possibly resulting in removal of the cells with highest concentration of activated caspases. One way of mitigating this could be to adjust caspase values proportionally with the number of dead cells, but this would have to be confirmed as being a real influence in the cell system before such adjustments were to be calculated.

5.2.4 Evaluating experimental conditions in relation to *in vivo* post-mortem conditions

There are some obvious differences in experimental conditions *in vitro* versus post-mortem conditions *in vivo*. First off, temperature was not changed in these *in vitro* experiments, but in

post-mortem treatment of meat the temperature is decreased gradually after slaughter. Secondly, available nutrition was not changed in this study, but in post-mortem muscle the nutrition delivery will stop because of the severed blood supply. The same is true for oxygen delivery to muscle, but *in vivo,* the oxygen concentration will decrease from physiological levels (about 3 % oxygen (Li et al., 2007)). In contrast, the experimental conditions *in vitro* had oxygen concentration of approximately 21 % before removal of oxygen. This could then give a higher relative toll on the *in vitro* cells than the ones *in vivo,* because of the larger difference in oxygen concentrations. The final factor to consider is pH in the stress medium opposed to pH in *in vivo* muscle. Both pH in meat and medium start at approximately 7 and is gradually decreased in muscle post-slaughter, but the reduction in pH is assumed to be lower under *in vitro* conditions, due to the relative higher concentration of medium to cells, giving a higher buffering capacity than in *in vivo*.

5.2.5 Reflections upon some of the analyses used for stress experiments

Since the process of apoptosis in satellite muscle cells has not been extensively studied in our laboratory prior to this study, there was a need to use some established methods and markers, known to be compatible with the satellite cell system. The most noticeable is the use of tubulin as control in western blot analysis of stress samples, since tubulin was shown to be affected by experimental conditions. Seeing that tubulin was depolymerized did not necessarily mean that the tubulin monomers were degraded. The tubulin antibody used in western blotting will still be able to recognize depolymerized tubulin monomers, resulting in a thorough detection of total tubulin in samples.

Another consideration was the use of internal control gene for real-time PCR in apoptosis experiments, which is not an easy task considering the vast amount of substrates for caspases and the overall impact of apoptosis. The TATA gene has been used as internal control in apoptosis studies of lung cells (Lin et al., 2010, Chen et al., 2004) and pancreatic cell lines (Yoon et al., 2011), showing that this gene is considered to be relatively unaffected by apoptosis in different cell types. This led to the conclusion that the TATA gene was sufficient as internal control for real-time PCR in stress experiments.

5.2.6 Relating findings to meat quality

Others have concluded that *in vivo* muscle cells die through apoptosis post-mortem (Becila et al., 2010, Cao et al., 2010), but there is still not any conclusive evidence regarding the impact of apoptosis on tenderness (Kemp and Parr, 2012). Even though the present study does not clarify if

apoptosis impacts tenderisation in a significant way, it brings forth more evidence to support the conclusions that muscle cells die through apoptosis when oxygen is removed and this may be a suitable method to elucidate what kind of genetic responses or which molecular mechanisms that is governing the process of apoptosis mediated tenderisation. In addition, this study shows that muscle cells can be able to change in response to environmental cues similar to the ones during the early stages post-mortem, and this should be taken into account when choosing post-mortem treatment of meat.

5.2.7 Summing up

Taken together, findings in the present study suggest that muscle cells induce apoptosis when oxygen is removed. Many early signs of apoptosis were observed, e.g. actin degradation, loss of mitochondrial membrane potential and concentration changes of Bcl2-like proteins. In the cell system used in this study, mitochondrial alterations seemed to be the governing factor for apoptosis.

5.3 Further research

Given that few studies have investigated bovine satellite cells and apoptosis *in vitro*, the present study can be seen as laying groundwork for further studies. To give a more complete picture of the entire process of post-mortem apoptosis, additional apoptosis markers should be examined, e.g. Apaf-1, cytochrome c leakage, chromatin remodelling and other supplementing caspases. These should also be examined at more points in time, to find the most crucial times after slaughter for optimising apoptotic impact on tenderisation.

The present study only altered available oxygen for the muscle cells, but there are many other post-mortem changes that could impact apoptosis processes, e.g. temperature, nutrition withdrawal, pH changes, and these factors should be taken into account and try to create a more dynamic environment when conducting further experiments.

Furthermore, the muscle cells may be more representative of *in vivo* meat if they are allowed to differentiate further. A way to do this could be to assess the time needed for the cells to express MHC, and use incubation times for differentiation before stress experiments that are slightly longer than the time needed for MHC expression.

6. Literature

ALBERTS, B., BRAY, D., LEWIS, J., RAFF, M., ROBERTS, K., and WATSON, J. D. 1989. *Molecular Biology of the Cell*. Second edition. Garland Publishing.

BARJOT, C., COTTEN, M. L., GOBLET, C., WHALEN, R. G. & BACOU, F. 1995. Expression of myosin heavy chain and of myogenic regulatory factor genes in fast or slow rabbit muscle satellite cell cultures. *J Muscle Res Cell Motil,* 16**,** 619-28.

BATEMAN, J. M. & MCNEILL, H. 2004. Temporal control of differentiation by the insulin receptor/tor pathway in Drosophila. *Cell,* 119**,** 87-96.

BECILA, S., HERRERA-MENDEZ, C. H., COULIS, G., LABAS, R., ASTRUC, T., PICARD, B., BOUDJELLAL, A., PELISSIER, P., BREMAUD, L. & OUALI, A. 2010. Postmortem muscle cells die through apoptosis. *European Food Research and Technology,* 231**,** 485-493.

BEERE, H. M. 2005. Death versus survival: functional interaction between the apoptotic and stress-inducible heat shock protein pathways. *J Clin Invest,* 115**,** 2633-9.

BERKES, C. A. & TAPSCOTT, S. J. 2005. MyoD and the transcriptional control of myogenesis. *Semin Cell Dev Biol,* 16**,** 585-95.

BISCHOFF, R. & HEINTZ, C. 1994. Enhancement of skeletal muscle regeneration. *Dev Dyn,* 201**,** 41-54.

BOLLAG, D. M. and EDELSTEIN S. J. 1991. *Protein Methods*. First edition. Wiley-Liss, Inc.

BOONEN, K. J., ROSARIA-CHAK, K. Y., BAAIJENS, F. P., VAN DER SCHAFT, D. W. & POST, M. J. 2009. Essential environmental cues from the satellite cell niche: optimizing proliferation and differentiation. *Am J Physiol Cell Physiol,* 296**,** C1338-45.

BOWKER, B. C., EASTRIDGE, J. S., PAROCZAY, E. W., CALLAHAN, J. A., and SOLOMON, M. B. 2010. Aging/Tenderization Mechanisms. In: F. TOLDRÁ ed. 2010. *Handbook of meat processing*. First edition, Wiley-Blackwell, pp. 87-104.

BRUCE, H. L. & BALL, R. O. 1990. Postmortem interactions of muscle temperature, pH and extension on beef quality. *J Anim Sci,* 68**,** 4167-75.

CANDE, C., COHEN, I., DAUGAS, E., RAVAGNAN, L., LAROCHETTE, N., ZAMZAMI, N. & KROEMER, G. 2002. Apoptosis-inducing factor (AIF): a novel caspase-independent death effector released from mitochondria. *Biochimie,* 84**,** 215-22.

CANET-AVILES, R. M., WILSON, M. A., MILLER, D. W., AHMAD, R., MCLENDON, C., BANDYOPADHYAY, S., BAPTISTA, M. J., RINGE, D., PETSKO, G. A. & COOKSON, M. R. 2004. The Parkinson's disease protein DJ-1 is neuroprotective due to cysteine-sulfinic acid-driven mitochondrial localization. *Proc Natl Acad Sci U S A,* 101**,** 9103-8.

CAO, J., SUN, W., ZHOU, G., XU, X., PENG, Z. & HU, Z. 2010. Morphological and biochemical assessment of apoptosis in different skeletal muscles of bulls during conditioning. *J Anim Sci,* 88**,** 3439-44.

CARLSON, M. E., HSU, M. & CONBOY, I. M. 2008. Imbalance between pSmad3 and Notch induces CDK inhibitors in old muscle stem cells. *Nature,* 454**,** 528-32.

CARLSSON, L. & THORNELL, L. E. 2001. Desmin-related myopathies in mice and man. *Acta Physiol Scand,* 171**,** 341-8.

CENCIARELLI, C., DE SANTA, F., PURI, P. L., MATTEI, E., RICCI, L., BUCCI, F., FELSANI, A. & CARUSO, M. 1999. Critical role played by cyclin D3 in the MyoD-mediated arrest of cell cycle during myoblast differentiation. *Mol Cell Biol,* 19**,** 5203-17.

CHEESEMAN, I. M. & DESAI, A. 2008. Molecular architecture of the kinetochore-microtubule interface. *Nat Rev Mol Cell Biol,* 9**,** 33-46.

CHEN, H. W., YU, S. L., CHEN, J. J., LI, H. N., LIN, Y. C., YAO, P. L., CHOU, H. Y., CHIEN, C. T., CHEN, W. J., LEE, Y. T. & YANG, P. C. 2004. Anti-invasive gene expression profile of curcumin in lung adenocarcinoma based on a high throughput microarray analysis. *Mol Pharmacol,* 65**,** 99-110.

COPELAND, R. A. 1994. *Methods for protein analysis: a practical guide to laboratory protocols.* First edition. Chapman & Hall.

CROMPTON, M. 1999. The mitochondrial permeability transition pore and its role in cell death. *Biochem J,* 341 (Pt 2)**,** 233-49.

DANOVIZ, M. E. & YABLONKA-REUVENI, Z. 2012. Skeletal muscle satellite cells: background and methods for isolation and analysis in a primary culture system. *Methods Mol Biol,* 798**,** 21-52.

DEVINE, C. E., WAHLGREN, N. M. & TORNBERG, E. 1999. Effect of rigor temperature on muscle shortening and tenderisation of restrained and unrestrained beef m. longissimus thoracicus et lumborum. *Meat Sci,* 51**,** 61-72.

DI CERA, E. 2009. Serine proteases. *IUBMB Life,* 61**,** 510-5.

DI LISA, F., BLANK, P. S., COLONNA, R., GAMBASSI, G., SILVERMAN, H. S., STERN, M. D. & HANSFORD, R. G. 1995. Mitochondrial membrane potential in single living adult rat cardiac myocytes exposed to anoxia or metabolic inhibition. *J Physiol,* 486 (Pt 1)**,** 1-13.

DOWNING, K. H. & NOGALES, E. 1998. Tubulin and microtubule structure. *Curr Opin Cell Biol,* 10**,** 16-22.

FAN, J., REN, H., JIA, N., FEI, E., ZHOU, T., JIANG, P., WU, M. & WANG, G. 2008. DJ-1 decreases Bax expression through repressing p53 transcriptional activity. *J Biol Chem,* 283**,** 4022-30.

FERNANDO, P., KELLY, J. F., BALAZSI, K., SLACK, R. S. & MEGENEY, L. A. 2002. Caspase 3 activity is required for skeletal muscle differentiation. *Proc Natl Acad Sci U S A,* 99**,** 11025-30.

FRANTZ, C., STEWART, K. M. & WEAVER, V. M. 2010. The extracellular matrix at a glance. *J Cell Sci,* 123**,** 4195-200.

GABAI, V. L., MABUCHI, K., MOSSER, D. D. & SHERMAN, M. Y. 2002. Hsp72 and stress kinase c-jun N-terminal kinase regulate the bid-dependent pathway in tumor necrosis factor-induced apoptosis. *Mol Cell Biol,* 22**,** 3415-24.

GOLL, D. E., THOMPSON, V. F., LI, H., WEI, W. & CONG, J. 2003. The calpain system. *Physiol Rev,* 83**,** 731-801.

GOTOH, T., TERADA, K., OYADOMARI, S. & MORI, M. 2004. hsp70-DnaJ chaperone pair prevents nitric oxide- and CHOP-induced apoptosis by inhibiting translocation of Bax to mitochondria. *Cell Death Differ,* 11**,** 390-402.

GREEN, D. R. 2011. The end and after: how dying cells impact the living organism. *Immunity,* 35**,** 441-4.

HANNULA, T. & PUOLANNE, E. 2004. The effect of cooling rate on beef tenderness: The significance of pH at 7 degrees C. *Meat Sci,* 67**,** 403-8.

HAUSER, D. N. & HASTINGS, T. G. 2013. Mitochondrial dysfunction and oxidative stress in Parkinson's disease and monogenic parkinsonism. *Neurobiol Dis,* 51**,** 35-42.

HAYFLICK, L. 1979. The cell biology of aging. *J Invest Dermatol,* 73**,** 8-14.

HERRERA-MENDEZ, C. H., BECILA, S., BOUDJELLAL, A. & OUALI, A. 2006. Meat ageing: Reconsideration of the current concept. *Trends in Food Science & Technology,* 17**,** 394-405.

HETTMER, S. & WAGERS, A. J. 2010. Muscling in: Uncovering the origins of rhabdomyosarcoma. *Nat Med,* 16**,** 171-3.

JIN, X., KIM, J. G., OH, M. J., OH, H. Y., SOHN, Y. W., PIAN, X., YIN, J. L., BECK, S., LEE, N., SON, J., KIM, H., YAN, C., WANG, J. H., CHOI, Y. J. & WHANG, K. Y. 2007. Opposite roles of MRF4 and MyoD in cell proliferation and myogenic differentiation. *Biochem Biophys Res Commun,* 364**,** 476-82.

JUÁREZ, M., ALDAI, N., LÓPEZ-CAMPOS, Ó., DUGAN, M. E. R., UTTARO , B., and AALHUS, J. L. 2012. Beef texture and Juiciness. In: Y. H. HUI ed. 2012. *Handbook of Meat and Meat Processing.* Second Edition, CRC Press, pp.177-207.

KANISICAK, O., MENDEZ, J. J., YAMAMOTO, S., YAMAMOTO, M. & GOLDHAMER, D. J. 2009. Progenitors of skeletal muscle satellite cells express the muscle determination gene, MyoD. *Dev Biol,* 332**,** 131-41.

KANNAN, K. & JAIN, S. K. 2000. Oxidative stress and apoptosis. *Pathophysiology,* 7**,** 153-163.

KEMP, C. M. & PARR, T. 2012. Advances in apoptotic mediated proteolysis in meat tenderisation. *Meat Sci,* 92**,** 252-9.

KERR, J. F., WYLLIE, A. H. & CURRIE, A. R. 1972. Apoptosis: a basic biological phenomenon with wide-ranging implications in tissue kinetics. *Br J Cancer,* 26**,** 239-57.

KOOHMARAIE, M. 1994. Muscle proteinases and meat aging. *Meat Sci,* 36**,** 93-104.

KOOHMARAIE, M. 1996. Biochemical factors regulating the toughening and tenderization processes of meat. *Meat Sci,* 43S1**,** 193-201.

KOOHMARAIE, M. & GEESINK, G. H. 2006. Contribution of postmortem muscle biochemistry to the delivery of consistent meat quality with particular focus on the calpain system. *Meat Sci,* 74**,** 34-43.

LARSON, R. E. 2004. Myosin motors. In: W. J. LENNARZ and M. D. LANE eds. 2004. *Encyclopedia of Biological Chemistry*. Elsevier, vol. 2, pp. 778-781.

LAVILLE, E., SAYD, T., MORZEL, M., BLINET, S., CHAMBON, C., LEPETIT, J., RENAND, G. & HOCQUETTE, J. F. 2009. Proteome changes during meat aging in tough and tender beef suggest the importance of apoptosis and protein solubility for beef aging and tenderization. *J Agric Food Chem,* 57**,** 10755-64.

LI, X., ZHU, L., CHEN, X. & FAN, M. 2007. Effects of hypoxia on proliferation and differentiation of myoblasts. *Med Hypotheses,* 69**,** 629-36.

LIN, S. Y., HSUEH, C. M., YU, S. L., SU, C. C., SHUM, W. Y., YEH, K. C., CHANG, G. C. & CHEN, J. J. 2010. HLJ1 is a novel caspase-3 substrate and its expression enhances UV-induced apoptosis in non-small cell lung carcinoma. *Nucleic Acids Res,* 38**,** 6148-58.

LIVAK, K. J. & SCHMITTGEN, T. D. 2001. Analysis of relative gene expression data using real-time quantitative PCR and the 2(-Delta Delta C(T)) Method. *Methods,* 25**,** 402-8.

LODISH, H., BALTIMORE, D., BERK, A., ZIPURSKY, S. L., MATSUDAIRA, P., and DARNELL, J. 1996. *Molecular cell biology.* Third edition, Scientific American Books.

LODISH, H., BERK, A., KAISER, C. A., KRIEGER, M., SCOTT, M. P., BRETSCHER, A., PLOEGH, H., and MATSUDAIRA, P. 2008. *Molecular cell biology.* Sixth edition, W.H. Freeman and Company.

MACEWAN, D. J. 2002. TNF ligands and receptors--a matter of life and death. *Br J Pharmacol,* 135**,** 855-75.

MAITI, S. and BAMBURG, J. R. 2004. Actin-capping and -severing proteins. In: W. J. LENNARZ and M. D. LANE eds. 2004. *Encyclopedia of Biological Chemistry*. Elsevier, vol. 1, pp. 19-26.

MALTIN, C., BALCERZAK, D., TILLEY, R. & DELDAY, M. 2003. Determinants of meat quality: tenderness. *Proc Nutr Soc,* 62**,** 337-47.

MARTIN, S. J., REUTELINGSPERGER, C. P., MCGAHON, A. J., RADER, J. A., VAN SCHIE, R. C., LAFACE, D. M. & GREEN, D. R. 1995. Early redistribution of plasma

membrane phosphatidylserine is a general feature of apoptosis regardless of the initiating stimulus: inhibition by overexpression of Bcl-2 and Abl. *J Exp Med,* 182**,** 1545-56.

MARTINAT, C., SHENDELMAN, S., JONASON, A., LEETE, T., BEAL, M. F., YANG, L., FLOSS, T. & ABELIOVICH, A. 2004. Sensitivity to oxidative stress in DJ-1-deficient dopamine neurons: an ES- derived cell model of primary Parkinsonism. *PLoS Biol,* 2**,** e327.

MEADOWS, E., CHO, J. H., FLYNN, J. M. & KLEIN, W. H. 2008. Myogenin regulates a distinct genetic program in adult muscle stem cells. *Dev Biol,* 322**,** 406-14.

MEHLEN, P., SCHULZE-OSTHOFF, K. & ARRIGO, A. P. 1996. Small stress proteins as novel regulators of apoptosis. Heat shock protein 27 blocks Fas/APO-1- and staurosporine-induced cell death. *J Biol Chem,* 271**,** 16510-4.

MILLER, M. F., CARR, M. A., RAMSEY, C. B., CROCKETT, K. L. & HOOVER, L. C. 2001. Consumer thresholds for establishing the value of beef tenderness. *J Anim Sci,* 79**,** 3062-8.

MILLS, J. C., STONE, N. L. & PITTMAN, R. N. 1999. Extranuclear apoptosis. The role of the cytoplasm in the execution phase. *J Cell Biol,* 146**,** 703-8.

MOSS, D. K., BETIN, V. M., MALESINSKI, S. D. & LANE, J. D. 2006. A novel role for microtubules in apoptotic chromatin dynamics and cellular fragmentation. *J Cell Sci,* 119**,** 2362-74.

MOSSER, D. D., CARON, A. W., BOURGET, L., MERIIN, A. B., SHERMAN, M. Y., MORIMOTO, R. I. & MASSIE, B. 2000. The chaperone function of hsp70 is required for protection against stress-induced apoptosis. *Mol Cell Biol,* 20**,** 7146-59.

MURRAY, T. V., MCMAHON, J. M., HOWLEY, B. A., STANLEY, A., RITTER, T., MOHR, A., ZWACKA, R. & FEARNHEAD, H. O. 2008. A non-apoptotic role for caspase-9 in muscle differentiation. *J Cell Sci,* 121**,** 3786-93.

MUSCHEL, R. J., BERNHARD, E. J., GARZA, L., MCKENNA, W. G. & KOCH, C. J. 1995. Induction of apoptosis at different oxygen tensions: evidence that oxygen radicals do not mediate apoptotic signaling. *Cancer Res,* 55**,** 995-8.

NATURE EDUCATION. 2010. *Figure 4: The structure of intermediate filaments.* Downloaded from: http://www.nature.com/scitable/topicpage/microtubules-and-filaments-14052932 (downloaded at : 30.04.2013).

NICHOLSON, D. W. 2000. From bench to clinic with apoptosis-based therapeutic agents. *Nature,* 407**,** 810-6.

NICHOLSON, D. W., NIOTERA, P., & MELINO, G. 2004. Caspases and cell death. In: W. J. LENNARZ and M. D. LANE eds. 2004. *Encyclopedia of Biological Chemistry*. Elsevier, vol. 1, pp. 319-327.

NOGALES, E. 2004. Tubulin and its isoforms. In: W. J. LENNARZ and M. D. LANE eds. 2004. *Encyclopedia of Biological Chemistry*. Elsevier, vol. 4, pp. 272-275.

ONO, S. 2010. Dynamic regulation of sarcomeric actin filaments in striated muscle. *Cytoskeleton (Hoboken),* 67**,** 677-92.

ORRENIUS, S., ZHIVOTOVSKY, B. & NICOTERA, P. 2003. Regulation of cell death: the calcium-apoptosis link. *Nat Rev Mol Cell Biol,* 4**,** 552-65.

OUALI, A., HERRERA-MENDEZ, C. H., COULIS, G., BECILA, S., BOUDJELLAL, A., AUBRY, L. & SENTANDREU, M. A. 2006. Revisiting the conversion of muscle into meat and the underlying mechanisms. *Meat Sci,* 74**,** 44-58.

OXYRASE, Inc. 2011. *EC (and EC/NS) Oxyrase® Enzyme System Product Insert.* Downloaded from: http://www.oxyrase.com/upload/documents/products/EC-Oxyrase/EC-Oxyrase_-_product_insert.pdf (downloaded at: 12.02.2013).

PAULIN, D. & LI, Z. 2004. Desmin: a major intermediate filament protein essential for the structural integrity and function of muscle. *Exp Cell Res,* 301**,** 1-7.

PROMEGA CORPORATION. 2012[a]. *Caspase-Glo® 3/7 Assay.* Downloaded from: http://no.promega.com/~/media/Files/Resources/Protocols/Technical%20Bulletins/101/Caspase-Glo%203%207%20Assay%20Protocol.pdf (downloaded at: 07.072013).

PROMEGA CORPORATION. 2012[b]. *Caspase-Glo® 9 Assay.* Downloaded from: http://no.promega.com/~/media/Files/Resources/Protocols/Technical%20Bulletins/101/Caspase-Glo%209%20Assay%20Protocol.pdf (downloaded at: 07.05.2013).

PROMEGA CORPORATION. 2012[c]. *CellTiter-Glo® Luminescent Cell Viability Assay.* Downloaded from: http://no.promega.com/~/media/Files/Resources/Protocols/Technical%20Bulletins/0/CellTiter%20Glo%20Luminescent%20Cell%20Viability%20Assay%20Protocol.pdf (downloaded at: 07.05.2013).

PURCHAS, R. W. & AUNGSUPAKORN, R. 1993. Further investigations into the relationship between ultimate pH and tenderness for beef samples from bulls and steers. *Meat Sci,* 34**,** 163-78.

PURCHAS, R. W., YAN, X. & HARTLEY, D. G. 1999. The influence of a period of ageing on the relationship between ultimate pH and shear values of beef m. longissimus thoracis. *Meat Sci,* 51**,** 135-41.

QIAGEN. 2006. *RNeasy® Mini Handbook. 4th ed.* Downloaded from: http://labs.fhcrc.org/fero/Protocols/RNeasy_Mini_Handbook.pdf (downloaded at: 19.10.2012).

RAVAGNAN, L., GURBUXANI, S., SUSIN, S. A., MAISSE, C., DAUGAS, E., ZAMZAMI, N., MAK, T., JAATTELA, M., PENNINGER, J. M., GARRIDO, C. & KROEMER, G. 2001. Heat-shock protein 70 antagonizes apoptosis-inducing factor. *Nat Cell Biol,* 3**,** 839-43.

RELAIX, F., MONTARRAS, D., ZAFFRAN, S., GAYRAUD-MOREL, B., ROCANCOURT, D., TAJBAKHSH, S., MANSOURI, A., CUMANO, A. & BUCKINGHAM, M. 2006. Pax3 and Pax7 have distinct and overlapping functions in adult muscle progenitor cells. *J Cell Biol,* 172**,** 91-102.

RUDNICKI, M. A., SCHNEGELSBERG, P. N., STEAD, R. H., BRAUN, T., ARNOLD, H. H. & JAENISCH, R. 1993. MyoD or Myf-5 is required for the formation of skeletal muscle. *Cell,* 75**,** 1351-9.

RØNNING, S. B., PEDERSEN, M. E., ANDERSEN, P. V. & HOLLUNG, K. 2013. The combination of glycosaminoglycans and fibrous proteins improve cell proliferation and early differentiation of bovine primary skeletal muscle cells. *Unpublished.*

SHACKELFORD, S. D., WHEELER, T. L. & KOOHMARAIE, M. 1999. Evaluation of slice shear force as an objective method of assessing beef longissimus tenderness. *J Anim Sci,* 77**,** 2693-9.

SIMON, M. M., REIKERSTORFER, A., SCHWARZ, A., KRONE, C., LUGER, T. A., JAATTELA, M. & SCHWARZ, T. 1995. Heat shock protein 70 overexpression affects the response to ultraviolet light in murine fibroblasts. Evidence for increased cell viability and suppression of cytokine release. *J Clin Invest,* 95**,** 926-33.

SLEE, E. A., ADRAIN, C. & MARTIN, S. J. 1999. Serial killers: ordering caspase activation events in apoptosis. *Cell Death Differ,* 6**,** 1067-74.

SMALL, J. V. & GIMONA, M. 1998. The cytoskeleton of the vertebrate smooth muscle cell. *Acta Physiol Scand,* 164**,** 341-8.

SMILEY, S. T., REERS, M., MOTTOLA-HARTSHORN, C., LIN, M., CHEN, A., SMITH, T. W., STEELE, G. D., JR. & CHEN, L. B. 1991. Intracellular heterogeneity in mitochondrial membrane potentials revealed by a J-aggregate-forming lipophilic cation JC-1. *Proc Natl Acad Sci U S A,* 88**,** 3671-5.

SMITH, M. I., HUANG, Y. Y. & DESHMUKH, M. 2009. Skeletal muscle differentiation evokes endogenous XIAP to restrict the apoptotic pathway. *PLoS One,* 4**,** e5097.

SUSIN, S. A., LORENZO, H. K., ZAMZAMI, N., MARZO, I., SNOW, B. E., BROTHERS, G. M., MANGION, J., JACOTOT, E., COSTANTINI, P., LOEFFLER, M., LAROCHETTE, N., GOODLETT, D. R., AEBERSOLD, R., SIDEROVSKI, D. P., PENNINGER, J. M. & KROEMER, G. 1999. Molecular characterization of mitochondrial apoptosis-inducing factor. *Nature,* 397**,** 441-6.

TASSIN, A. M., MARO, B. & BORNENS, M. 1985. Fate of microtubule-organizing centers during myogenesis in vitro. *J Cell Biol,* 100**,** 35-46.

VAUX, D. L. 2004. Bax and Bcl2 cell death enhancers and inhibitors. In: W. J. LENNARZ and M. D. LANE eds. 2004. *Encyclopedia of Biological Chemistry*. Elsevier, vol. 1, pp. 152-154.

VIGNON, X., BEAULATON, J. & OUALI, A. 1989. Ultrastructural localization of calcium in post-mortem bovine muscle: a cytochemical and X-ray microanalytical study. *Histochem J,* 21**,** 403-11.

YABLONKA-REUVENI, Z., and DAY, K. 2011. Skeletal Muscle Stem Cells in the Spotlight: The Satellite Cell. In: I.S. COHEN and G.R. GAUDETTE eds. 2011. *Regenerating the Heart,* Stem Cell Biology and Regenerative Medicine. Springer Science + Business Media**,** pp. 173-200.

YABLONKA-REUVENI, Z., RUDNICKI, M. A., RIVERA, A. J., PRIMIG, M., ANDERSON, J. E. & NATANSON, P. 1999. The transition from proliferation to differentiation is delayed in satellite cells from mice lacking MyoD. *Dev Biol,* 210**,** 440-55.

YANG, Y. B., PANDURANGAN, M. & HWANG, I. 2012. Changes in proteolytic enzymes mRNAs and proteins relevant for meat quality during myogenesis and hypoxia of primary bovine satellite cells. *In Vitro Cell Dev Biol Anim,* 48**,** 359-68.

YOON, K., LEE, S. O., CHO, S. D., KIM, K., KHAN, S. & SAFE, S. 2011. Activation of nuclear TR3 (NR4A1) by a diindolylmethane analog induces apoptosis and proapoptotic genes in pancreatic cancer cells and tumors. *Carcinogenesis,* 32**,** 836-42.

YUN, Z., LIN, Q. & GIACCIA, A. J. 2005. Adaptive myogenesis under hypoxia. *Mol Cell Biol,* 25**,** 3040-55.

ZHANG, K., SHA, J. & HARTER, M. L. 2010. Activation of Cdc6 by MyoD is associated with the expansion of quiescent myogenic satellite cells. *J Cell Biol,* 188**,** 39-48.